

# Efficient numerical solution of a simple discretization of Biot's model

Carmen Rodrigo (carmenr@unizar.es)

Instituto Universitario de Matemáticas y Aplicaciones (IUMA), Departamento de Matemática Aplicada,  
Universidad de Zaragoza

*Premio a la Investigación de la Academia 2025. Sección de Exactas*

## Abstract

This work presents a simple and efficient approach for the numerical solution of the single-phase flow problem in deformable porous media. To this end, Biot's model is derived from basic principles of fluid and solid mechanics, and the numerical challenges associated with its discretization and the solution of the resulting algebraic systems are discussed. Piecewise linear finite element methods are considered as one of the simplest discretization strategies for this problem, and a suitable stabilization technique is introduced to ensure uniform stability properties and a monotone discrete scheme. To solve the algebraic systems arising from the stabilized discretization, efficient decoupled solvers are reviewed and theoretically analyzed. In particular, we propose an iterative coupling method and a non-iterative sequential method for solving the resulting stabilized scheme. The efficiency and robustness of both the discretization and the solution approaches are demonstrated.

## 1 Introduction

The focus of this work is the efficient numerical simulation of multiphysics problems involving single phase flow in a deformable porous medium within the context of the Biot theory of poroelasticity. This continuum theory studies the behaviour of a porous media consisting of an elastic matrix containing interconnected pores filled by fluids and it is based on the fact that the

presence of a freely moving fluid within the pores modifies the mechanical response of the media. In particular, the theory postulates that when a porous material is subjected to stress, the resulting matrix deformation causes volumetric changes in the pores. Since the pores are filled by fluid, the presence of the fluid not only acts as a stiffener of the material, but also leads to the flow of the pore fluid between regions of higher and lower pore pressure.

The first work accounting for the interrelation of pore fluid and the quasi-static deformation of soils was by Terzaghi [78]. However, his work was based on experimental work and on a one-dimensional consolidation model. Further on, his theory was generalized by Biot, who established the general theory of poroelasticity through several pioneering papers [14, 15]. This theory originally was developed for soil mechanics especially for consolidation problems, since most rocks are porous materials which are generally saturated by different fluid phases. The mechanical behavior of porous rocks is affected by variations of fluid pressures, and, at the same time, the flow kinetics of each fluid phase is influenced by rock deformation. Thus, Biot's theory soon became crucial in geophysical applications related to enhanced oil recovery, injection/pumping operations into geological formations, oil and gas-hydrate exploration or seismic monitoring of CO<sub>2</sub> storage, among others. Since then, many researchers have contributed to its further development, and new applications have benefited from the extensive development of the poroelastic theory. In particular, such a theory found its applications in biology, medicine and biomedical engineering for the description of different anatomical structures as vertebrate discs or cornea, biological tissues as cartilage, different organs as the brain or the heart, for example, becoming fundamental in important applications as the study of tumor growth, heart perfusion, brain mechanics, for instance. Nowadays, Biot's model is extensively studied, both theoretically and computationally, since it is essential in the understanding of a wide range of applications in different branches of science and engineering.

The existence, uniqueness, and regularity of the solutions of Biot's equations have been widely studied, see the works by Showalter [72], Zenisek [84] and Phillips and Wheeler [63], and the references therein. The mathematical models for flow in deformable porous media consist of coupled, and possibly nonlinear, partial differential equations, and therefore, analytical solutions of these poroelastic models in closed form are only possible for very particular and restricted cases. For example, some of these benchmark models with analytical solution are Terzaghi [78], Mandel [52, 1] and Barry and Mercer [9] problems. So, the numerical simulation of Biot's models are of great interest to scientists and engineers, since reliable numerical methods for solving poroelastic problems are needed for the accurate solution of multiphysics phenomena appearing in a great variety of fields. It is therefore necessary to develop discrete numerical

models suitable for computer solution. The discrete model arises from the discretization of the continuous model by different techniques, and gives rise to a large set of algebraic equations per time step. The main focus is then twofold: first, to choose appropriate discretization schemes that provide numerical solutions whose behavior resembles that of the real problems and, second, to design suitable large-scale computational algorithms for their efficient solution.

Discretization schemes for Biot's equations have been widely studied. Finite difference methods, which are simple and easy to implement have been analyzed for such a problem [33, 34]. Cell-centered finite volume methods are predominant in the numerical simulation of flow problems [8, 23], as in the industry standard simulation software Eclipse (by Schlumberger and Stars by CMG). These methods have been traditionally combined with finite element methods for dealing with the coupling between flow and mechanics, but recently, a compatible finite volume scheme for coupled hydromechanic flows in porous media was proposed by Jan Martin Nordbotten (MPSA) [58, 59, 60]. This approach is a generalization of the multi-point flux approximation (MPFA) for the scalar conservation equation to mechanical deformation, and has the advantage that the same data structures are used in both the flow problem and the mechanics part. The finite element method, however, provides flexibility to handle complex geometries and has a better developed convergence and stability theory, and thus, has been widely considered to approximate the solution of complex poromechanics problems. See for example the monograph by Lewis and Schrefler [50], where the authors provide an exhaustive compilation of their work on finite element schemes for poroelastic problems, the references therein and some other more recent works such as [46, 49, 70, 82].

One of the main challenges in the numerical simulation of poroelasticity problems is to avoid the appearance of numerical instabilities in the approximation of the pressure variable [5, 26, 28, 37, 66, 83]. Problems where the solution is smooth are satisfactorily solved by standard discretization schemes, but when strong pressure gradients appear, strong nonphysical oscillations can appear in the numerical approximation of the fluid pressure. Such instabilities occur in presence of low-permeability materials and/or when a small time step is used at the beginning of the consolidation process. The oscillations can be removed if considering very fine target grids, or when imposing stability restrictions between the space and time discretization parameters (see [5, 79]). Such techniques, however, can result in prohibitively expensive computational methods and therefore are not practical for real applications. There are different points of view about the nature of these instabilities in the literature. In a finite element framework, they are often attributed to the violation of the inf-sup condition, or the lack of monotonicity of the scheme, in general. These oscillations can be minimized (but not completely alleviated

without reducing the spatial mesh size) if inf-sup stable finite element methods are used. In several papers, Murad and Loula [55, 56, 57] analyzed the behavior of stable discretizations for the classical two-field formulation. The inf-sup condition, however, is not a sufficient requirement to guarantee numerical solutions free of oscillations, as seen in [5] and [69] where Taylor-Hood elements [76] (continuous piecewise quadratic functions for the approximation of the displacement and continuous piecewise linear functions for the pressure), and the so-called MINI element [7] (continuous piecewise linear functions for both variables, enriching the space for displacements with the element bubble functions) are considered, respectively. Other authors have proposed other techniques to avoid the appearance of non-physical oscillations as for example the use of least-squares mixed finite-element methods [45, 77], different combinations of continuous and discontinuous Galerkin methods and mixed finite-element methods [63, 64, 65], nonconforming finite-element methods [41], or a new formulation of the problem including the so-called total pressure variable [61]. These non-physical oscillations can be also eliminated by appropriate stabilization techniques, adding, in particular, certain stabilization terms to the Galerkin formulation of the problem, see for example [13] and [5, 69].

Following the numerical discretization of the problem, the other important aspect of computational schemes is the design of efficient solvers for the solution of the arising large-scale linear system of algebraic equations that has to be solved at each time step. Such linear systems are usually ill-conditioned and difficult to solve in practice. Incorporation of more detailed physics and geometry into the mathematical models requires the use of efficient numerical algorithms, becoming the design of these methods a crucial step to allow the numerical simulation of realistic problems. In particular, the solution of the large linear systems of equations arising from the discretization of Biot's model is the most time-consuming part when real simulations are performed, and often constitute a major bottleneck in coupled flow and geomechanics simulations. For this reason, during the last years, significant effort has been focused on designing efficient iterative solution methods for these problems. Poroelastic models are computationally complex to retain the characteristics of the underlying physical processes, and their numerical simulation becomes expensive, time consuming and difficult. In fact, up to our knowledge, there are no commercial packages readily available to solve these type of coupled problems. The classical approach is to consider separate software modules for mechanics and flow calculations, implemented in both a sequential or iterative setting. In the literature, there are mainly three different approaches for solving the coupling between geomechanics and flow in a porous media: the fully implicit schemes, the iterative coupling methods and the explicit approach.

On the one hand, the so-called monolithic, fully coupled or fully implicit methods solve

the coupled flow and geomechanics system simultaneously in a monolithic manner, that is, simultaneously for all the unknowns on each time level. This strategy allows to take larger time steps and enjoys excellent stability properties. Its main disadvantage, however, lies in their high computational cost due to the need of solving complex ill-conditioned linear systems. Also, it does not allow to use well tested robust versions of individual model components, and loses some flexibility since it does not permit to use larger time steps for the geomechanics than for the flow subproblem. Within this framework, Krylov-type iterative methods and/or multigrid algorithms are frequently used, due to their scalability and good parallel performance. In the case of Krylov iterative methods, an essential ingredient is to design an effective preconditioner which could address both the ill-conditioning and the strong coupling nature of the governing equations, and thus accelerate the convergence of Krylov subspace methods. Some examples can be found in [3, 2, 71, 12, 27, 18, 22, 36, 39, 67]. Multigrid methods are known to have optimal complexity for solving many numerical problems. However, in practice their performance in solving individual problems varies significantly. Multigrid methods for the transport of a fluid in porous media are well understood, but the black-box multigrid treatment of the poroelasticity equations is less common. Within the multigrid framework, the focus is on the design of appropriate smoothers to deal with the saddle point type character of the resulting system. Different smoothers have been proposed in the literature for dealing with Biot's problem within a multigrid framework. Coupled Vanka smoothers, decoupled distributive relaxations, Uzawa type smoothers and other decoupled relaxations based on iterative coupling methods have been successfully applied for such a problem [32, 31, 51, 35, 4].

An alternative to the monolithic methods is a sequential approach in which the fully coupled system is broken into subproblems (flow and mechanics problems) that are solved one after the other. This fully explicit coupling approach is a very simple scheme which allows much flexibility in the implementation and has a low computational cost, however it pays maybe the price of a less accurate numerical solution by using the same discretization parameters and might also only be conditionally stable. This approach has the advantage that established numerical methods and existing software and simulators can be used for each of the subproblems. In this way, it results quite attractive in practice since smaller linear systems need to be solved in order to obtain the solution for the whole coupled poroelastic system. Due to the appealing advantages of these methods, intensive research is currently being carried out in this direction. Some examples can be found in [48, 19, 85, 6, 21, 68].

A sequential approach may be iterated further at each time step until the solution converges within a specified tolerance. This is commonly known as an iteratively coupled approach, and

the solution obtained is, in principle, the same as the that obtained using a monolithic approach. Thus, for solving Biot's model, the iterative coupling schemes solve, on each time step, either the flow or the mechanic part, followed by the solution of the other subproblem, repeating this process until a converged solution within a prescribed tolerance is obtained [44]. This approach has the same advantages of the previous decoupling solution methods regarding their flexibility, since two different existing codes (one for the fluid flow and one for the geomechanics) can be used for solving the whole coupled poroelastic problem. Special care, however, is needed for their appropriate design, avoiding a slow convergence of the coupling schemes. In addition, these splitting techniques can be also considered as preconditioners for the fully implicit approach, see [29, 30]. The most commonly used iterative coupling methods are the drained and undrained splittings, which solve the mechanical problem first, and the fixed-strain and fixed-stress splittings, which solve the flow problem first [42, 43]. In particular, the fixed stress splitting is the most used in practice due to its unconditional convergence, and it has been widely analyzed [16, 17, 20, 35, 53, 74]. In this scheme, the flow problem is firstly solved fixing the volumetric mean total stress, and then the mechanics part is solved from the values obtained at the previous flow step. This method, however, requires the choice of a certain stabilization parameter which has to be sufficiently large in order to ensure the convergence of the iteration [17].

There is another important issue to take into account in the numerical simulation of poroelastic problems. The corresponding mathematical models involve a large number of physical parameters, and the values of some of such parameters may vary over orders of magnitude in different applications. For example, the value of the permeability can typically range from  $10^{-9}$  to  $10^{-21}$   $\text{m}^2$  in geophysical applications [47, 80], and from  $10^{-14}$  to  $10^{-16}$   $\text{m}^2$  in biophysical applications such as in the modeling of soft tissue or bone [11, 73, 75]. The Poisson ratio can take values varying from 0.1 to 0.5 depending on the degree of incompressibility of the media. Therefore, the large variation of values of these physical parameters makes important to consider discretizations that are uniformly stable, independently of the values of the physical parameters, and solution methods that perform well under such large variations of the parameters. When a numerical method satisfies such properties, it is called parameter-robust method and the design of such type of methods has been the focus of study of the scientific community for the past few years (see for example [2, 38, 47, 71, 70]).

In this work, we gather some numerical techniques that we proposed to deal with the issues raised above by using a very simple numerical scheme for poroelastic problems. More concretely, piecewise linear finite element methods are considered as the simplest discretization scheme for this problem, together with an appropriate stabilization to avoid non-physical oscillations, and

two different decoupled strategies for solving the resulting systems of algebraic equations are derived from the stabilized scheme and theoretically analyzed. Thus, the structure of the paper is as follows. In Section 2 we derive the governing equations for Biot's model, while in Section 3 we introduce the considered discretization together with the proposed stabilization technique and a discussion about the numerical issue arising with the appearance of non-physical oscillations. Section 4 is devoted to derive the decoupled solvers from the stabilized formulation of the discrete problem previously introduced. In particular, in Section 4.1 an iterative coupling approach is presented and in Section 4.2 a non-iterative sequential scheme is derived. Finally, in Section 5 some conclusions are drawn.

## 2 Biot's model. Mathematical formulation

Biot's model is built from the basic principles of fluid and solid mechanics. In particular it couples the governing equations for fluid flow and solid deformation in poroelastic media, taking into account the equilibrium and mass conservation principles, as well as Darcy's law.

We assume a linearly elastic, homogeneous and isotropic porous medium, saturated by a Newtonian fluid. The model is based on the interaction between a solid skeleton and a freely moving pore fluid, which dictates the choice of the main quantities to deal with: the solid displacement vector  $\mathbf{u}$ , which tracks the movement of the solid matrix, and the fluid velocity vector  $\mathbf{q}$ , denoting the rate of fluid volume that crosses a unit area of porous solid. This latter is related to the gradient of the pore pressure  $p$  by the following linear relationship

$$(1) \quad \mathbf{q} = -\frac{\kappa}{\mu_f} (\nabla p - \rho_f \mathbf{g})$$

which is known as Darcy's law, and where  $\kappa$  is the permeability of the soil,  $\mu_f$  is the viscosity of the fluid,  $\rho_f$  is the density of the fluid and  $\mathbf{g}$  is the gravitational acceleration vector. The strain tensor  $\varepsilon(\mathbf{u})$  is introduced to follow the deformation of the solid skeleton by the following compatibility equation

$$(2) \quad \varepsilon(\mathbf{u}) = \frac{1}{2} (\nabla \mathbf{u} + \nabla^T \mathbf{u}).$$

For a stressed body to remain in equilibrium, all the forces acting on it must balance each other. This requirement leads to the equilibrium equation, given by

$$(3) \quad \operatorname{div} \boldsymbol{\sigma} + \mathbf{f} = 0,$$

where  $\boldsymbol{\sigma}$  is the stress tensor, and  $\mathbf{f}$  is the density of applied body forces. There are three reasons by which a change of volume of a porous medium can appear: due to compression of the fluid, due to compression of the grains or due to a rearrangement of the grains. The two first mechanisms are controlled by the fluid and solid compressibility, respectively. The latter one is related to the principle of effective stress. This notion was introduced by Terzaghi, who established that the total stress is carried in part by the fluid and in part by the soil structure. The part of the total stress that is not carried by the fluid is called the effective stress, and actually this is the stress applied to the grains of the porous medium. Thus, rearrangement of the soil grains is caused by changes in the effective stress and not by changes in the total stress. Therefore, the total stress  $\boldsymbol{\sigma}$  can be split up into the sum of the effective stress, usually denoted by  $\boldsymbol{\sigma}'$ , and the pore pressure  $p$ , that is,

$$(4) \quad \boldsymbol{\sigma} = \boldsymbol{\sigma}' + \alpha p \mathbf{I},$$

where parameter  $\alpha$  is the Biot coefficient and depends on the compressibilities of the solid  $c_s$  and porous medium  $c_b$  such that  $\alpha = 1 - \frac{c_s}{c_b}$ . In continuum mechanics, the effective stress tensor and the strain tensor are fundamentally related through the material's constitutive equations, which characterize its mechanical behavior under loading. In the case of linear elasticity, as it is our case, this relationship is linear and is described by Hooke's law, which expresses the stress components as linear functions of the strain components via the material's elasticity tensor. For isotropic materials, this relation can be written as

$$(5) \quad \boldsymbol{\sigma}' = \lambda \text{tr}(\boldsymbol{\varepsilon}(\mathbf{u})) \mathbf{I} + 2\mu \boldsymbol{\varepsilon}(\mathbf{u}),$$

where  $\lambda$  and  $\mu$  are the so-called Lamé coefficients, which can be computed in terms of the Young modulus,  $E$ , and the Poisson ratio,  $\nu$ , as follows:

$$\lambda = \frac{E\nu}{(1-2\nu)(1+\nu)} \quad \text{and} \quad \mu = \frac{E}{1+2\nu}.$$

In order to describe the amount of fluid in a deformable porous media, the so-called fluid content  $\xi$  is defined as

$$(6) \quad \xi = \frac{p}{\beta} + \alpha \text{div } \mathbf{u},$$

where  $\beta$  is known as the Biot modulus. Note that the first part in the right-hand side of this

equation measures the change in the amount of fluid as a result of the change in the pore pressure  $p$  under constant volumetric strain  $\nabla \cdot \mathbf{u}$ . In turn, the second part  $\alpha \nabla \cdot \mathbf{u}$  measures the amount of fluid content due to deformation of the porous medium. The fluid mass conservation equation is given by

$$(7) \quad \frac{\partial \xi}{\partial t} + \operatorname{div} \mathbf{q} = g,$$

where the source term  $g$  represents a forced fluid extraction or injection process. Substituting (6) into (7), we obtain the

$$(8) \quad \frac{\partial}{\partial t} \left( \frac{1}{\beta} p + \alpha \operatorname{div} \mathbf{u} \right) + \operatorname{div} \mathbf{q} = g.$$

Thus, the system of equations governing the consolidation process is given by the equilibrium equation for the porous medium, obtained combining (3) and (4), and the continuity equation (8),

$$(9) \quad -\operatorname{div} \boldsymbol{\sigma}' + \alpha \nabla p = \mathbf{f},$$

$$(10) \quad \frac{\partial}{\partial t} \left( \frac{1}{\beta} p + \alpha \operatorname{div} \mathbf{u} \right) + \operatorname{div} \mathbf{q} = g.$$

Finally, for linear isotropic materials the stress tensor  $\boldsymbol{\sigma}$  is given by Hooke's law (5) and the Darcy velocity  $\mathbf{q}$  relates to the pressure through Darcy's law (1). Under these assumptions, this set of partial differential equations can be written as a coupled system in terms of the displacements of the solid matrix  $\mathbf{u}$  and the pore pressure  $p$ , giving rise to the so-called displacement-pressure formulation or two-field formulation for Biot's model, which is given by the following system of partial differential equations (PDEs):

$$(11) \quad -\nabla (2\mu \boldsymbol{\varepsilon}(\mathbf{u}) + \lambda \nabla \cdot \mathbf{u}) + \alpha \nabla p = \mathbf{f},$$

$$(12) \quad \frac{1}{\beta} \frac{\partial p}{\partial t} + \alpha \nabla \cdot \frac{\partial \mathbf{u}}{\partial t} - \nabla \cdot (K(\nabla p - \rho_f \mathbf{g})) = g,$$

on a space-time domain  $\Omega \times (0, T_f]$ , where  $\Omega \subset \mathbb{R}^d$ ,  $d \leq 3$ ,  $T_f > 0$ , where  $K$  denotes the hydraulic conductivity which is given by the quotient between the permeability  $\kappa$  and the viscosity of the fluid  $\mu_f$ , i.e.  $K = \frac{\kappa}{\mu_f}$ .

To complete the formulation of a well-posed problem, we need to include appropriate boundary and initial conditions. For example, we can consider a part of the boundary which is free to drain and where a traction is applied, and other part that is assumed to be rigid and impermeable, that

is,

$$(13) \quad \begin{aligned} p &= 0, & \boldsymbol{\sigma} \mathbf{n} &= \mathbf{t}, & & \text{on } \Gamma_t, \\ \mathbf{u} &= \mathbf{0}, & K (\nabla p - \rho_f \mathbf{g}) \cdot \mathbf{n} &= 0, & & \text{on } \Gamma_c, \end{aligned}$$

where  $\mathbf{n}$  is the unit outward normal to the boundary  $\Gamma$ , which is split into two disjoint subsets  $\Gamma_t$  and  $\Gamma_c$  with non null measure such that  $\Gamma = \Gamma_t \cup \Gamma_c$ .

For the initial time  $t = 0$  the following condition is assumed,

$$(14) \quad \left( \frac{1}{\beta} p + \alpha \nabla \cdot \mathbf{u} \right) (x, 0) = 0, \quad x \in \Omega.$$

### 3 Discrete scheme. Numerical issues

To present the variation formulation of problem (11)-(14), we first introduce appropriate function spaces. Let  $L^2(\Omega)$  be the Hilbert space of square integrable scalar valued functions defined on  $\Omega$ , with inner product

$$(p, q) = \int_{\Omega} p q \, dx, \quad p, q \in L^2(\Omega),$$

and let us consider  $H^1(\Omega)$  which denotes the subspace of  $L^2(\Omega)$  of functions with weak first derivatives in  $L^2(\Omega)$ . Then, we define the following Sobolev spaces for displacements and pressure variables:

$$(15) \quad \mathbf{V} = \{ \mathbf{u} \in (H^1(\Omega))^d \mid \mathbf{u} = \mathbf{0} \text{ on } \Gamma_c \},$$

$$(16) \quad Q = \{ q \in H^1(\Omega) \mid q = 0 \text{ on } \Gamma_t \}.$$

By considering the bilinear forms corresponding to the elasticity and the scaled Laplacian operators, that is,

$$a(\mathbf{u}, \mathbf{v}) = 2\mu \int_{\Omega} \boldsymbol{\varepsilon}(\mathbf{u}) : \boldsymbol{\varepsilon}(\mathbf{v}) \, d\Omega + \lambda \int_{\Omega} \operatorname{div} \mathbf{u} \operatorname{div} \mathbf{v} \, d\Omega, \quad a_p(p, q) = \int_{\Omega} K \nabla p \cdot \nabla q \, d\Omega,$$

we can write the variational formulation of the two-field formulation of Biot's problem as follows:

Find  $(\mathbf{u}(t), p(t)) \in C^1([0, T_f]; \mathbf{V}) \times C^1([0, T_f]; Q)$  such that

$$(17) \quad a(\mathbf{u}, \mathbf{v}) - \alpha(p, \operatorname{div} \mathbf{v}) = (\mathbf{f}, \mathbf{v}), \quad \forall \mathbf{v} \in \mathbf{V},$$

$$(18) \quad \frac{1}{\beta} (\partial_t p, q) + \alpha(\operatorname{div} \partial_t \mathbf{u}, q) + a_p(p, q) = (g, q) + (K \rho_f \mathbf{g}, \nabla q), \quad \forall q \in Q.$$

with the initial condition,

$$(19) \quad \left( \frac{1}{\beta} p(0) + \alpha \nabla \cdot \mathbf{u}(0), q \right) = 0, \quad \forall q \in L^2(\Omega).$$

Notice that in (18) the time derivative is denoted by  $\partial_t$  for compactness of notation.

Now, we consider the finite element approximation of problem (17)-(19) and, in particular, linear finite element methods are used to approximate both displacement and pressure unknowns, as previously commented. Let  $\mathcal{T}_h$  be a partition of  $\Omega \subset \mathbb{R}^d$  consisting of triangles ( $d = 2$ ) or tetrahedrons ( $d = 3$ ). Thus, we choose the following finite-element pair of spaces  $\mathbf{V}_h \times \mathcal{Q}_h$  to approximate the displacements and the pressure, respectively, where

$$\begin{aligned} \mathbf{V}_h &= \{ \mathbf{v}_h \in (H^1(\Omega))^d \mid \mathbf{v}_h|_T \in (P_1)^d, \forall T \in \mathcal{T}_h, \mathbf{v}_h|_{\Gamma_c} = \mathbf{0} \}, \\ \mathcal{Q}_h &= \{ p_h \in H^1(\Omega) \mid p_h|_T \in P_1, \forall T \in \mathcal{T}_h, p_h|_{\Gamma_t} = 0 \}, \end{aligned}$$

where  $P_1$  denotes the space of scalar piecewise linear functions on  $\mathcal{T}_h$ . To discretize in time, we use the backward Euler method on a uniform partition of the time interval  $(0, T_f]$ ,  $t_j = j\tau$ ,  $j = 0, \dots, N$ , with time-step  $\tau = \frac{T_f}{N}$ , leading to the following fully-discrete scheme:

For given initial values  $(\mathbf{u}_h^0, p_h^0) \in \mathbf{V}_h \times \mathcal{Q}_h$ , for  $n = 1, 2, \dots, N$ , find  $(\mathbf{u}_h^n, p_h^n) \in \mathbf{V}_h \times \mathcal{Q}_h$  such that

$$(20) \quad a(\mathbf{u}_h^n, \mathbf{v}_h) - \alpha(p_h^n, \operatorname{div} \mathbf{v}_h) = (\mathbf{f}_h^n, \mathbf{v}_h), \quad \forall \mathbf{v}_h \in \mathbf{V}_h,$$

$$(21) \quad \frac{1}{\beta} (\bar{\partial}_t p_h^n, q_h) + \alpha (\operatorname{div} \bar{\partial}_t \mathbf{u}_h^n, q_h) + a_p(p_h^n, q_h) = (g_h^n, q_h), \quad \forall q_h \in \mathcal{Q}_h,$$

where  $\bar{\partial}_t p_h^n := (p_h^n - p_h^{n-1})/\tau$ ,  $\bar{\partial}_t \mathbf{u}_h^n := (\mathbf{u}_h^n - \mathbf{u}_h^{n-1})/\tau$ , and where  $(g_h^n, q_h)$  includes the discrete counterpart of the right-hand side  $(g, q) + (K\rho_f \mathbf{g}, \nabla q)$  of (18).

By introducing operators notation, and establishing the following correspondences among operators and the bilinear forms:

$$(22)$$

$$a(\mathbf{u}_h, \mathbf{v}_h) \rightarrow A, \quad -\alpha(p_h, \operatorname{div} \mathbf{v}_h) \rightarrow G, \quad \alpha(\operatorname{div} \mathbf{u}_h, q_h) \rightarrow D, \quad a_p(p_h, q_h) \rightarrow A_p, \quad (p_h, q_h) \rightarrow M.$$

we can rewrite the discrete problem (20)-(21) in the following block form:

$$(23) \quad \mathcal{A} \begin{pmatrix} \mathbf{u} \\ p \end{pmatrix} = \begin{pmatrix} \mathbf{f} \\ g \end{pmatrix}, \quad \text{with} \quad \mathcal{A} = \begin{pmatrix} A & G \\ D & \tau A_p + \beta^{-1} M \end{pmatrix}.$$

Note that  $D = -G^T$  by definition.

### 3.1 Numerical difficulties. Non-physical oscillations

As previously commented in the introduction, the pressure field may exhibit non-physical oscillations when some standard combinations of finite elements are used to discretize the problem. This is the case, for example, when linear finite element methods are used to approximate both displacement and pressure unknowns. In particular, such an unstable behavior may occur when the porous material has a low permeability and/or when a small time step is used at the beginning of the consolidation process. To illustrate this behavior, below we present some examples. First, we consider a very simple one-dimensional problem: the Terzaghi's problem. After that, a modification of such a simple problem, in which we have included an intermediate layer with a very low permeability is considered. Finally, a two-dimensional benchmark problem is analyzed too.

#### 3.1.1 EXAMPLE 1 - TERZAGHI PROBLEM

The Terzaghi problem models a column of a porous medium with height,  $H$ , saturated by an incompressible fluid, bounded by impermeable and rigid lateral walls and bottom, and supporting a load  $\sigma_0$  on the top boundary which is free to drain (see Figure 1(a)). This results in the following one-dimensional version of model (11)-(12):

$$(24) \quad \begin{aligned} -\frac{\partial}{\partial x} \left( (\lambda + 2\mu) \frac{\partial u}{\partial x} \right) + \frac{\partial p}{\partial x} &= 0, \\ \frac{\partial}{\partial t} \left( \frac{\partial u}{\partial x} \right) - \frac{\partial}{\partial x} \left( K \frac{\partial p}{\partial x} \right) &= 0, \end{aligned} \quad (x, t) \in (0, H) \times (0, T_f],$$

where for simplicity we have fixed  $\alpha = 1$  and  $1/\beta = 0$ . This system is supplemented with the following boundary and initial conditions,

$$\begin{aligned} (\lambda + 2\mu) \frac{\partial u}{\partial x}(0, t) &= \sigma_0, \quad p(0, t) = 0, \quad t \in (0, T_f], \\ u(H, t) &= 0, \quad K \frac{\partial p}{\partial x}(H, t) = 0, \quad t \in (0, T_f], \\ \frac{\partial u}{\partial x}(x, 0) &= 0, \quad x \in [0, H]. \end{aligned}$$

A uniform partition of spatial domain  $\Omega = (0, H)$  with mesh size  $h$  is considered, and the backward Euler method is chosen for discretization in time, together with the spatial P1-P1 method.

When discretizing using linear finite elements for both displacement and pressure, non-

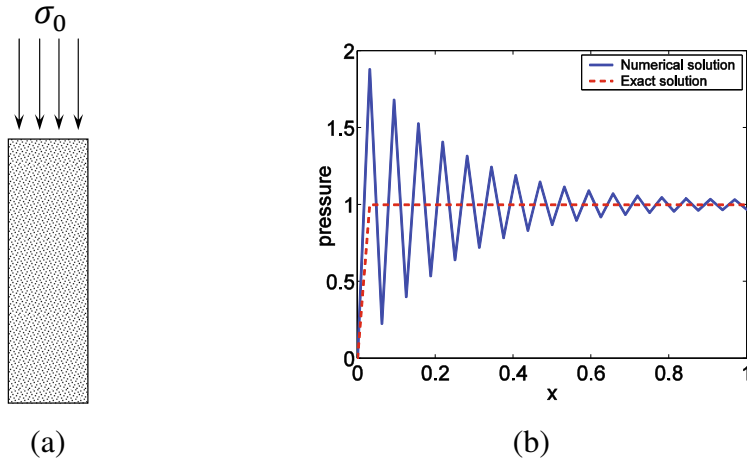


Figure 1: (a) Domain for Terzaghi problem and (b) non-physical oscillations in the numerical solution of the pressure field for Terzaghi problem.

physical oscillations are observed in the numerical solution of the pressure even for this simple problem. This can be seen In Figure 1(b), where we display the numerical solution obtained for the pressure field at the final time  $T_f = 0.1$ , taking the hydraulic conductivity  $K = 10^{-6}$ ,  $\lambda + 2\mu = 1$ , Biot coefficient  $\alpha = 1$ , and a mesh size  $h = 1/32$ .

### 3.1.2 EXAMPLE 2 - TWO-LAYER PROBLEM

Non-physical oscillations in the pressure field may also appear when a low-permeability is assumed in a region of the domain. In order to illustrate this, we consider a porous material on which a low-permeable layer ( $K = 10^{-8}$ ) is placed between two layers with unit permeability ( $K = 1$ ), as shown in Figure 2(a). The boundary of the squared domain is split into two disjoint subsets  $\Gamma_1$  and  $\Gamma_2$  on which we assume the following boundary conditions: on the top, which is free to drain ( $p = 0$ ), a uniform load is applied, that is,  $\sigma' \mathbf{n} = \mathbf{g}$  with  $\mathbf{g} = (0, -1)^t$ , on  $\Gamma_1$ , whereas at the sides and bottom of the domain that are rigid ( $\mathbf{u} = \mathbf{0}$ ) the boundary is impermeable, that is,  $\nabla p \cdot \mathbf{n} = 0$  on  $\Gamma_2$ . This test can be reduced to a one-dimensional problem, and, therefore, it is enough to analyze the numerical solutions corresponding to one vertical line in the domain as displayed in Figure 2(a).

When linear finite elements for displacements and pressure are considered, the approximation for the pressure field that is obtained by using 32 elements in the grid is shown in Figure 2(b). There, we can observe that strong spurious oscillations appear in the part of the domain corresponding to the low-permeable layer.

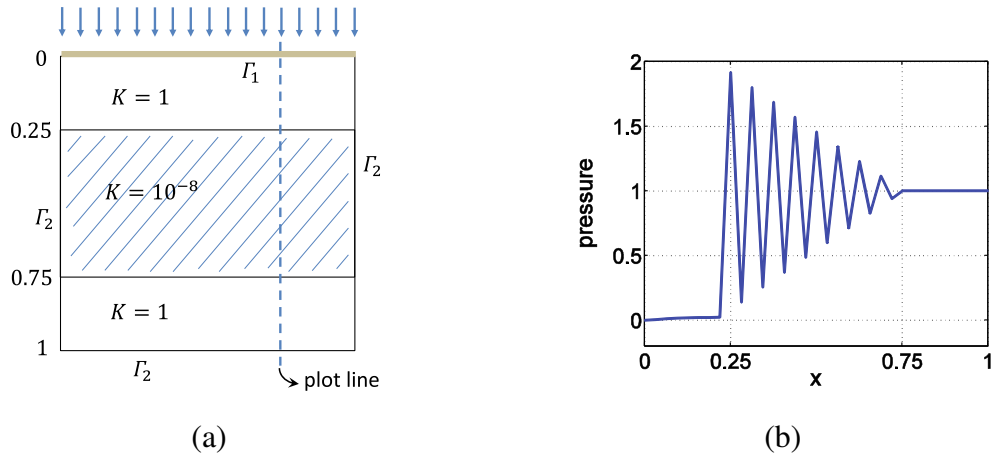


Figure 2: (a) Domain for the two-layer problem and (b) non-physical oscillations in the numerical solution of the pressure for the two-layer problem.

### 3.1.3 EXAMPLE 3 - BARRY & MERCER PROBLEM

As third example we consider a well-known poroelastic benchmark test on a finite two-dimensional domain which is called Barry & Mercer's problem [9]. It models the behavior of a rectangular uniform porous material  $[0, a] \times [0, b]$  drained on all sides, and with zero tangential displacements assumed on the whole boundary, in which a pulsating point source is considered. Such a point-source corresponds to a sine wave and is given by  $f(t) = 2\nu \delta_{(x_0, y_0)} \sin(\nu t)$ , where  $\nu = \frac{(\lambda + 2\mu)K}{ab}$  and  $\delta_{(x_0, y_0)}$  is the Dirac delta at the point  $(x_0, y_0)$ . In Figure 3(a), the computational domain and the boundary conditions of the problem are depicted.

In particular, we consider the unit square domain  $(0, 1) \times (0, 1)$ , and the following values of the material parameters:  $E = 10^5$ ,  $\nu = 0.1$ ,  $\alpha = 1$ ,  $\beta = 10^8$  and  $K = 10^{-6}$ . The source is positioned at the point  $(1/4, 1/4)$ , and a right triangular grid of mesh size  $h = 2^{-6}$  is used for the simulations. Fluid pressure oscillations for the Barry and Mercer's problem can be observed by considering standard P1-P1 discretizations. In Figure 3(b), we show the numerical solutions obtained for the pressure field at a final time  $T_f = 10^{-4}$ , with only one time step. We observe that non-physical oscillations appear in the numerical pressure near the source-point.

### 3.2 Stabilization scheme

In order to deal with the numerical issues presented above in the previous section, by using one of the simplest discretization that one can consider for the two-field formulation of Biot's model (linear finite elements for both displacements and pressure unknowns), we propose a way to

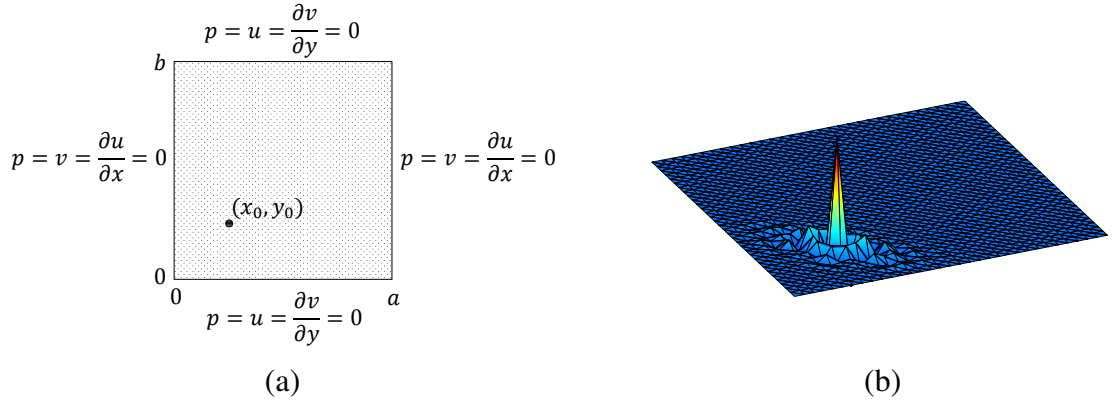


Figure 3: (a) Computational domain and boundary conditions for the Barry and Mercer's source problem, and (b) numerical solution of the pressure for the Barry & Mercer problem (at the final time  $T_f = 10^{-4}$  with hydraulic conductivity  $K = 10^{-6}$ , Poisson ratio  $\nu = 0.1$ , and mesh spacing  $h = 1/64$ ).

stabilize the arising discrete problem. The main idea is to add the term  $L \frac{\partial p}{\partial t}$  to both sides in the flow equation (12), and discretizing the two new terms in a different way: we use mass matrix for the discretization of the term in the right hand side and the row-sum lumped mass matrix on the left hand side term. This leads to the following discrete variational formulation:

$$(25) \quad a(\mathbf{u}_h^n, \mathbf{v}_h) - \alpha(p_h^n, \operatorname{div} \mathbf{v}_h) = (\mathbf{f}_h^n, \mathbf{v}_h), \quad \forall \mathbf{v}_h \in \mathbf{V}_h,$$

$$(26) \quad \frac{1}{\beta} (\bar{\partial}_t p_h^n, q_h) + \alpha(\operatorname{div} \bar{\partial}_t \mathbf{u}_h^n, q_h) + a_p(p_h^n, q_h) + L(\bar{\partial}_t p_h^n, q_h)_0 - L(\bar{\partial}_t p_h^n, q_h) = (g_h^n, q_h), \quad \forall q_h \in \mathcal{Q}_h,$$

where  $(\cdot, \cdot)_0$  is an approximation of the  $L^2(\Omega)$  inner product defined by mass lumping, *i.e.*, for continuous functions  $p$  and  $q$  defined on  $\bar{\Omega}$ , we have

$$(p, q)_0 = \sum_{T \in \mathcal{T}_h} \int_T (pq)_I dx = \sum_{T \in \mathcal{T}_h} \frac{|T|}{d+1} \sum_{j=1}^{d+1} (pq)(P_{T,j}),$$

where  $(pq)_I$  denotes the linear interpolant of the continuous function  $(pq)$  and  $P_{T,j}$  are the coordinates of the  $j$ -th vertex of  $T \in \mathcal{T}_h$ . In (26),  $L$  is a parameter appropriately chosen to remove the non-physical oscillations. In particular, for the considered P1-P1 discretization, the parameter

is chosen as

$$(27) \quad L = \frac{1}{\beta} + \frac{3\alpha^2}{2\left(\lambda + \frac{2\mu}{d}\right)}.$$

The choice of this parameter is done in the one-dimensional case in the way that it is the optimal value to provide a monotone scheme that eliminates the oscillations without inducing extra diffusion effects in the numerical solution.

**Remark 3.1.** *The considered stabilized scheme is identical to the one given in [5] for one-dimensional problems. This scheme has been widely cited in the porous media community and was theoretically analyzed in [69], where it was observed numerically that oscillations were eliminated also in problems with two and three spatial dimensions, though supporting theory for such observation is missing. The stabilization considered in this work also leads to a monotone scheme, and it has several advantages with respect to the techniques proposed in [5, 69]. Some of these benefits are the fact that the stabilization parameter  $L$  does not depend on the mesh size, and that it has been derived for any value of the storage coefficient. In addition, as it is shown in next sections, the current stabilization scheme provides a way to derive decoupled solvers for Biot's model which are convergent without the need to introduce other stabilization terms (as it is the case for the well-known fixed stress split method).*

Following the notation introduced in (22) and (23), the fully-discrete stabilized scheme (25)-(26) can be written in block form as follows:

$$(28) \quad \mathcal{A}_{stab} \begin{pmatrix} \mathbf{u} \\ p \end{pmatrix} = \begin{pmatrix} f \\ g \end{pmatrix}, \quad \text{with} \quad \mathcal{A}_{stab} = \begin{pmatrix} A & G \\ D & \tau A_p + \beta^{-1}M + L(M_l - M) \end{pmatrix},$$

where  $M$  and  $M_l$  the mass matrix and the lumped mass matrix, respectively.

Next, we prove the stabilized scheme's stability in order to demonstrate the well-posedness of the discrete problem (25)-(26). With this purpose, we show a relationship between the stabilization technique studied in [69] and the stabilized scheme considered in this work.

**Lemma 3.2.** *The difference between the lumped mass matrix  $M_l$  and the mass matrix  $M$  on a simplicial grid, that is  $M_l - M$ , is spectrally equivalent to the scaled stiffness matrix  $h^2 L_p$ , where  $\langle h^2 L_p p, q \rangle := \sum_{T \in \mathcal{T}} h_T^2 \int_T |\nabla p|^2$ , that is,*

$$(29) \quad C_1 \langle (M_l - M)p, q \rangle \leq \langle h^2 L_p p, q \rangle \leq C_2 \langle (M_l - M)p, q \rangle.$$

*Proof.* Let  $p$  and  $q$  be piecewise linear continuous functions, then we have the following

$$\begin{aligned}\langle Mp, q \rangle &= \sum_{T \in \mathcal{T}_h} \int_T pq \, d\mathbf{x}, \\ \langle M_l p, q \rangle &= \sum_{T \in \mathcal{T}_h} \int_T (pq)_I \, d\mathbf{x}.\end{aligned}$$

Let us define  $Z = (M_l - M)$ , then we can write,

$$\langle Zp, q \rangle = \sum_{T \in \mathcal{T}_h} \langle Z_T p_T, q_T \rangle,$$

where, for a fixed  $T \in \mathcal{T}_h$ ,  $\langle Z_T p_T, q_T \rangle$  is the difference between the integrals in the definitions of  $M_l$  and  $M$  and  $p_T \in \mathbb{R}^{d+1}$  is the vector that represents the degrees of freedom of  $p(x)$  with components  $\{p_{T,k}\}_{k=1}^{d+1}$  on  $T$ .

Evaluating the integrals on  $T \in \mathcal{T}_h$  and using the Poincaré inequality for convex domains [10, Theorem 3.2], we have that

$$\frac{1}{d+1} \langle Z_T p_T, p_T \rangle = \int_T \left( p - \frac{1}{|T|} \int_T p \, d\mathbf{x} \right)^2 \, d\mathbf{x} \leq \frac{h_T^2}{\pi^2} \int_T |\nabla p|^2 \, d\mathbf{x}.$$

On the other hand, from [81, Equations (2.3)-(2.4)], we obtain the bound

$$(30) \quad h_T^2 \int_T |\nabla p|^2 \, d\mathbf{x} \leq \frac{c_T |T|}{2} \sum_{j=1}^{d+1} \sum_{k=1}^{d+1} (p_{T,j} - p_{T,k})^2 = c_T (d+1)(d+2) \langle Z_T p_T, p_T \rangle,$$

with  $c_T := \max_{\substack{1 \leq j, k \leq (d+1) \\ j \neq k}} \left\{ \frac{h_T^2}{|h_j| |h_k|} \right\}$ , where  $h_j$  (and similarly  $h_k$ ) is the distance from the vertex

$P_{T,j}$  ( $P_{T,k}$  for  $h_k$ ) to the face of  $T$  opposite to this vertex. Summing over all elements  $T \in \mathcal{T}_h$  shows that  $Z = (M_l - M)$  is spectrally equivalent to the scaled stiffness matrix corresponding to the Laplace operator  $h^2 L_p$ , and we obtain the spectral equivalence in (29).  $\square$

Consequently, we can derive an inf-sup condition that guarantees the well-posedness of the stabilized discrete problem.

**Theorem 3.3.** *The following weak inf-sup condition*

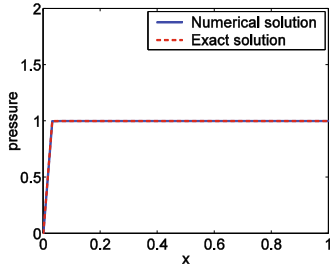
$$(31) \quad \sup_{\mathbf{w}_h \in \mathbf{V}_h} \frac{(q, \operatorname{div} \mathbf{w}_h)}{\|\mathbf{w}_h\|_A} \geq \eta \frac{1}{\sqrt{\lambda + 2\mu/d}} \|q\| - \epsilon \frac{1}{\sqrt{\lambda + 2\mu/d}} h \|\nabla q\|, \quad \forall q \in Q_h,$$

where  $h = \max_T h_T$  and  $\eta > 0$  and  $\epsilon > 0$  are constants that do not depend on the mesh size or the physical parameters, is fulfilled.

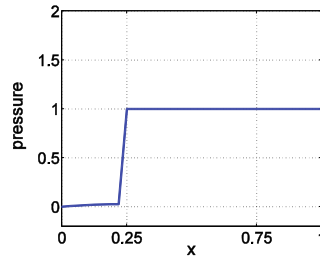
*Proof.* The proof of the inf-sup condition follows from the application of Lemma 3.2 and the theoretical results derived in [69, 3, 71]. In particular, the inf-sup condition is similar to the one shown in [69, Theorem 1].  $\square$

Summarizing, the stabilization terms and the stabilization parameters are derived in a mathematically consistent manner, and the computationally convenient equal-order interpolation of all the field variables has been shown to be stable.

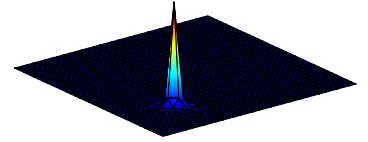
Finally, we demonstrate that the stabilized scheme (25)-(26) provides numerical solutions that are free of non-physical oscillations. With this purpose, we solve the problems considered in the three examples presented above in Section 3.1 by using the proposed scheme. The numerical solution of the pressure for each of these problems is depicted in Figure 4, and we can observe that the spurious oscillations are completely eliminated for all the cases.



(a) Example 1



(b) Example 2



(c) Example 3

Figure 4: Numerical solution of the pressure field for the examples introduced in Section 3.1: (a) Terzaghi problem, (b) Two-layer problem and (c) Barry & Mercer problem.

## 4 Efficient decoupled solvers

An alternative to the classical monolithic or fully coupled schemes is the use of decoupled solvers, which address the coupled poroelastic problem by splitting it into a sequence of subproblems that

can be solved separately. In such approaches, the flow and mechanics equations are treated independently, with information exchanged between the subproblems through an iterative or staggered procedure. This partitioned strategy can significantly reduce computational costs and facilitate the use of existing solvers optimized for each physical field.

In the next two sections, we present iterative and non-iterative coupling methods for solving Biot's model by using simple piecewise linear finite elements for both displacement and pressure variables. These solution methods are straightforwardly derived from the stabilized scheme introduced in Section 3.2.

#### 4.1 Iterative coupling method

From the considered stabilized discrete scheme (25)-(26), we straightforwardly obtain a sequential-implicit method, which is similar to the fixed-stress splitting method, but with the advantage that no additional stabilization of the iteration is required for convergence. The idea is first to solve the flow problem and then the mechanics, and iterate until a converged solution is obtained. Therefore, at each time level  $t_n$ , we consider the following iterative method for the solution of (25)-(26):

Given the initial guess for the coupling iteration at time  $t_n$ ,  $\mathbf{u}_h^{n,0} = \mathbf{u}_h^{n-1}$  and  $p_h^{n,0} = p_h^{n-1}$ , the algorithm provides a sequence of approximations  $(\mathbf{u}_h^{n,i}$  and  $p_h^{n,i})$ ,  $i \geq 1$ , as follows:

**Step 1:** Given  $(\mathbf{u}_h^{n,i-1}, p_h^{n,i-1}) \in \mathbf{V}_h \times Q_h$ , find  $p_h^{n,i} \in Q_h$  such that:

$$(32) \quad \frac{1}{\beta} \left( \frac{p_h^{n,i} - p_h^{n-1}}{\tau}, q_h \right) + L \left( \frac{p_h^{n,i} - p_h^{n-1}}{\tau}, q_h \right)_0 + a_p(p_h^{n,i}, q_h) = -\alpha \left( \operatorname{div} \frac{\mathbf{u}_h^{n,i-1} - \mathbf{u}_h^{n-1}}{\tau}, q_h \right) + L \left( \frac{p_h^{n,i-1} - p_h^{n-1}}{\tau}, q_h \right) + (g_h^n, q_h), \quad \forall q_h \in Q_h,$$

**Step 2:** Given  $p_h^{n,i} \in Q_h$ , find  $\mathbf{u}_h^{n,i} \in \mathbf{V}_h$  such that

$$(33) \quad a(\mathbf{u}_h^{n,i}, \mathbf{v}_h) = \alpha(p_h^{n,i}, \operatorname{div} \mathbf{v}_h) + (\mathbf{f}_h^n, \mathbf{v}_h), \quad \forall \mathbf{v}_h \in \mathbf{V}_h.$$

The previous algorithm is based on the following splitting of  $\mathcal{A}_{stab}$ ,

$$\mathcal{A}_{stab} = \begin{pmatrix} A & G \\ D & C \end{pmatrix} = \begin{pmatrix} A & G \\ 0 & \tau A_p + \beta^{-1} M + L M_l \end{pmatrix} - \begin{pmatrix} 0 & 0 \\ -D & L M \end{pmatrix}.$$

Although we can prove the robust convergence of algorithm (32)-(33), we aim to optimize the convergence of the iterative coupling method. With this purpose, we have to distinguish two different cases: the case when  $\beta^{-1}$  is very close to zero and a more general fluid regime that implies a bigger value of  $\beta^{-1}$ . For simplicity in the presentation, we will focus on the first case, that is, the proposed approach is presented in detail for the case in which the storage coefficient  $\beta^{-1}$  is close to zero and therefore the appropriate stabilization parameter given in (27) reduces to  $L = \frac{3\alpha^2}{2\left(\lambda + \frac{2\mu}{d}\right)}$ . At the end of the section, its extension to a more general case which includes the regime with larger values of  $1/\beta$  is briefly introduced.

In this case, in order to optimize the convergence of the scheme, we introduce a parameter  $\gamma$  to split the term corresponding to  $M_l$  and have more flexibility when studying the convergence. In this way, the proposed iterative method at each time step  $t_n$  is defined as:

Given the initial guess for the coupling iteration at time  $t_n$ ,  $\mathbf{u}_h^{n,0} = \mathbf{u}_h^{n-1}$  and  $p_h^{n,0} = p_h^{n-1}$ , the algorithm provides a sequence of approximations  $(\mathbf{u}_h^{n,i}$  and  $p_h^{n,i})$ ,  $i \geq 1$ , as follows:

**Step 1:** Given  $(\mathbf{u}_h^{n,i-1}, p_h^{n,i-1}) \in \mathbf{V}_h \times Q_h$ , find  $p_h^{n,i} \in Q_h$  such that:

$$(34) \quad \begin{aligned} & \frac{1}{\beta} \left( \frac{p_h^{n,i} - p_h^{n-1}}{\tau}, q_h \right) + \gamma L \left( \frac{p_h^{n,i} - p_h^{n-1}}{\tau}, q_h \right)_0 + a_p(p_h^{n,i}, q_h) = -\alpha \left( \operatorname{div} \frac{\mathbf{u}_h^{n,i-1} - \mathbf{u}_h^{n-1}}{\tau}, q_h \right) \\ & + L \left( \frac{p_h^{n,i-1} - p_h^{n-1}}{\tau}, q_h \right) + (\gamma - 1) L \left( \frac{p_h^{n,i-1} - p_h^{n-1}}{\tau}, q_h \right)_0 + (g_h^n, q_h), \quad \forall q_h \in Q_h, \end{aligned}$$

**Step 2:** Given  $p_h^{n,i} \in Q_h$ , find  $\mathbf{u}_h^{n,i} \in \mathbf{V}_h$  such that

$$(35) \quad a(\mathbf{u}_h^{n,i}, \mathbf{v}_h) = \alpha(p_h^{n,i}, \operatorname{div} \mathbf{v}_h) + (\mathbf{f}_h^n, \mathbf{v}_h), \quad \forall \mathbf{v}_h \in \mathbf{V}_h.$$

Equivalently, the iterative method can be written by means of the following splitting of  $\mathcal{A}_{stab}$ ,

$$(36) \quad \mathcal{A}_{stab} = \begin{pmatrix} A & G \\ 0 & \tau A_p + \beta^{-1}M + \gamma LM_l \end{pmatrix} - \begin{pmatrix} 0 & 0 \\ -D & LM + (\gamma - 1)LM_l \end{pmatrix}.$$

Then, our aim is to demonstrate the convergence of the iterative method presented in (34)-(35). In addition, it is important to show a robust convergence with respect to the physical and discretization parameters of the model. With this purpose, let us define  $e_u^i = \mathbf{u}_h^{n,i} - \mathbf{u}_h^n$  and  $e_p^i = p_h^{n,i} - p_h^n$  as the errors at iteration  $i$  for the displacements and for the pressure, respectively, and in the next result we present the corresponding error estimates.

**Theorem 4.1.** *The iterative method given in (34)-(35) is convergent for any parameters  $\gamma \in (2/3, 2]$  such that  $\gamma L = \omega \frac{\alpha^2}{(\lambda+2\mu/d)} \geq \frac{\alpha^2}{(\lambda+2\mu/d)}$ , i.e.,  $\omega \geq 1$ . Additionally,*

$$(37) \quad \|e_p^i\|^2 + \frac{|1-\gamma|}{\gamma} \|e_p^i\|_Z^2 \leq \frac{1}{1 + \frac{\eta^2}{\omega(1+2\theta^*)}} \left( \|e_p^i\|^2 + \frac{|1-\gamma|}{\gamma} \|e_p^{i-1}\|_Z^2 \right),$$

where  $\theta^* \geq \frac{\epsilon^2 C_2 \gamma}{4\omega(\gamma-|1-\gamma|)}$  is a root of the following quadratic equation

$$(38) \quad q_2(\theta) := \left[ \frac{2(\gamma - |1-\gamma|)}{\gamma} \right] \theta^2 + \left[ \frac{\gamma - |1-\gamma|}{\gamma} - \frac{\eta^2 |1-\gamma|}{2\omega\gamma} - \frac{\epsilon^2 C_2}{2\omega} \right] \theta - \frac{\epsilon^2 C_2}{4\omega} = 0.$$

Here,  $\eta > 0$  is the constant appearing in the weak inf-sup condition (31), and  $C_2$  is the constant for the upper bound of the spectral equivalence condition (29).

*Proof.* By subtracting equations (25) and (35) tested with  $v_h = e_u^{i-1} \in V_h$  and equations (26) and (34) tested with  $q_h = e_p^i \in Q_h$ , adding all together, and using that  $M_l - M = Z$ , we obtain the following:

$$a(e_u^i, e_u^{i-1}) + \frac{1}{\beta} \|e_p^i\|^2 + \tau \|e_p^i\|_{A_p}^2 + \gamma L(e_p^i - e_p^{i-1}, e_p^i) + \gamma L(e_p^i, e_p^i)_Z + (1-\gamma)L(e_p^{i-1}, e_p^i)_Z = 0,$$

which implies the following inequality by using a polarization identity and Young's inequality:

$$(39) \quad \begin{aligned} & \frac{1}{2} \|e_u^i\|_A^2 + \frac{1}{2} \|e_u^{i-1}\|_A^2 + \frac{1}{\beta} \|e_p^i\|^2 + \tau \|e_p^i\|_{A_p}^2 + \frac{\gamma L}{2} \|e_p^i\|^2 + \frac{\gamma L}{2} \|e_p^i - e_p^{i-1}\|^2 + \\ & + \left( \gamma - \frac{|1-\gamma|}{2} \right) L \|e_p^i\|_Z^2 \leq \frac{\gamma L}{2} \|e_p^{i-1}\|^2 + \frac{1}{2} \|e_u^i - e_u^{i-1}\|_A^2 + \frac{|1-\gamma|}{2} L \|e_p^{i-1}\|_Z^2. \end{aligned}$$

As a first step, we take the difference between equations (35) and (25) evaluated at iteration  $i$  and  $i - 1$ , tested with  $\mathbf{v}_h = e_{\mathbf{u}}^i - e_{\mathbf{u}}^{i-1}$  which yields:

$$\begin{aligned} \|e_{\mathbf{u}}^i - e_{\mathbf{u}}^{i-1}\|_A^2 &= \alpha(e_p^i - e_p^{i-1}, \nabla \cdot (e_{\mathbf{u}}^i - e_{\mathbf{u}}^{i-1})) \leq \alpha \|e_p^i - e_p^{i-1}\| \|\nabla \cdot (e_{\mathbf{u}}^i - e_{\mathbf{u}}^{i-1})\| \\ &\leq \frac{\alpha}{\sqrt{\lambda + 2\mu/d}} \|e_p^i - e_p^{i-1}\| \|e_{\mathbf{u}}^i - e_{\mathbf{u}}^{i-1}\|_A, \end{aligned}$$

where we use the Cauchy-Schwarz inequality and the fact that  $a(\mathbf{u}, \mathbf{u}) \geq (\lambda + \frac{2\mu}{d}) \|\nabla \cdot \mathbf{u}\|^2$ . Thus,

$$(40) \quad \|e_{\mathbf{u}}^i - e_{\mathbf{u}}^{i-1}\|_A \leq \frac{\alpha}{\sqrt{\lambda + 2\mu/d}} \|e_p^i - e_p^{i-1}\|.$$

From the weak inf-sup condition (31), we know that, for any given  $e_p^i$ , there exists  $\mathbf{w}_h \in V_h$ , such that

$$(e_p^i, \operatorname{div} \mathbf{w}_h) \geq \left( \eta \frac{1}{\sqrt{\lambda + 2\mu/d}} \|e_p^i\| - \epsilon \frac{1}{\sqrt{\lambda + 2\mu/d}} h \|\nabla e_p^i\| \right) \|\mathbf{w}_h\|_A, \quad \|\mathbf{w}_h\|_A = \|e_p^i\|.$$

Thus, as a second step, subtracting equations (35) and (25) and testing with  $\mathbf{v}_h = \mathbf{w}_h$  we derive that,

$$\begin{aligned} &\alpha \left( \eta \frac{1}{\sqrt{\lambda + 2\mu/d}} \|e_p^i\| - \epsilon \frac{1}{\sqrt{\lambda + 2\mu/d}} h \|\nabla e_p^i\| \right) \|\mathbf{w}_h\|_A \leq \alpha (e_p^i, \operatorname{div} \mathbf{w}_h) \\ &= a(e_{\mathbf{u}}^i, \mathbf{w}_h) \leq \|e_{\mathbf{u}}^i\|_A \|\mathbf{w}_h\|_A, \end{aligned}$$

which implies

$$\|e_{\mathbf{u}}^i\|_A \geq \eta \frac{\alpha}{\sqrt{\lambda + 2\mu/d}} \|e_p^i\| - \epsilon \frac{\alpha}{\sqrt{\lambda + 2\mu/d}} h \|\nabla e_p^i\|.$$

Now, by using Young's inequality with constant  $\theta > 0$ , we obtain

$$(41) \quad \|e_{\mathbf{u}}^i\|_A^2 \geq \frac{\eta^2}{1 + 2\theta} \frac{\alpha^2}{\lambda + 2\mu/d} \|e_p^i\|^2 - \frac{\epsilon^2}{2\theta} \frac{\alpha^2}{\lambda + 2\mu/d} h^2 \|\nabla e_p^i\|^2.$$

At the end, substituting the inequalities obtained in (40) and (41) back into (39), dropping the

$\frac{1}{2}\|e_u^{i-1}\|_A^2$ ,  $\frac{1}{\beta}\|e_p^i\|^2$ , and  $\tau\|e_p^i\|_{A_p}^2$  terms, we arrive at

$$\begin{aligned} & \left( \frac{1}{2} \frac{\eta^2}{1+2\theta} \frac{\alpha^2}{\lambda+2\mu/d} + \frac{\gamma L}{2} \right) \|e_p^i\|^2 + \frac{\gamma L}{2} \|e_p^i - e_p^{i-1}\|^2 + \left( \gamma - \frac{|1-\gamma|}{2} \right) L \|e_p^i\|_Z^2 \\ & \leq \frac{\gamma L}{2} \|e_p^{i-1}\|^2 + \frac{1}{2} \frac{\alpha^2}{\lambda+2\mu/d} \|e_p^i - e_p^{i-1}\|^2 + \frac{|1-\gamma|}{2} L \|e_p^{i-1}\|_Z^2 + \frac{\epsilon^2 C_2}{4\theta} \frac{\alpha^2}{\lambda+2\mu/d} \|e_p^i\|_Z^2. \end{aligned}$$

By applying the theorem's hypothesis  $\gamma L = \omega \frac{\alpha^2}{\lambda+2\mu/d} \geq \frac{\alpha^2}{\lambda+2\mu/d}$ , i.e.,  $\omega \geq 1$ , we have

$$\left( \frac{1}{2} \frac{\eta^2}{1+2\theta} \frac{\gamma}{\omega} + \frac{\gamma}{2} \right) \|e_p^i\|^2 + \left( \left(1 - \frac{\epsilon^2 C_2}{4\omega\theta}\right) \gamma - \frac{|1-\gamma|}{2} \right) \|e_p^i\|_Z^2 \leq \frac{\gamma}{2} \|e_p^{i-1}\|^2 + \frac{|1-\gamma|}{2} \|e_p^{i-1}\|_Z^2.$$

Finally, in order to guarantee the convergence, we require that,

$$\left(1 - \frac{\epsilon^2 C_2}{4\omega\theta}\right) \gamma - \frac{|1-\gamma|}{2} \geq \frac{|1-\gamma|}{2} \implies \theta \geq \frac{\epsilon^2 C_2 \gamma}{4\omega(\gamma - |1-\gamma|)}.$$

Next, we try to find  $\theta = \theta^* \geq \frac{\epsilon^2 C_2 \gamma}{4\omega(\gamma - |1-\gamma|)}$  such that

$$\frac{\left(1 - \frac{\epsilon^2 C_2}{4\omega\theta}\right) \gamma - \frac{|1-\gamma|}{2}}{\frac{1}{2} \frac{\eta^2}{1+2\theta} \frac{\gamma}{\omega} + \frac{\gamma}{2}} = \frac{|1-\gamma|}{\gamma}.$$

Direct calculations show that  $\theta^* \geq \frac{\epsilon^2 C_2 \gamma}{4\omega(\gamma - |1-\gamma|)}$  should be the positive root of the quadratic equation (38). Since  $\frac{2(\gamma - |1-\gamma|)}{\gamma} > 0$  for  $\gamma \in (\frac{2}{3}, 2]$ , the existence of  $\theta^*$  is verified by the positiveness of the discriminant, and the fact that  $q_2\left(\frac{\epsilon^2 C_2 \gamma}{4\omega(\gamma - |1-\gamma|)}\right) \leq 0$ . Therefore, we have

$$\left( \frac{\eta^2 \gamma}{2\omega(1+2\theta^*)} + \frac{\gamma}{2} \right) \left( \|e_p^i\|^2 + \frac{|1-\gamma|}{\gamma} \|e_p^i\|_Z^2 \right) \leq \frac{\gamma}{2} \left( \|e_p^i\|^2 + \frac{|1-\gamma|}{\gamma} \|e_p^{i-1}\|_Z^2 \right),$$

from where we can derive result (37) in the theorem and then complete the proof.  $\square$

Summarizing, we have demonstrated the convergence of the iterative method (34)-(35) for a set of values of parameter  $\gamma$ , in particular for any parameter  $\gamma \in (2/3, 2]$  such that  $\gamma L$  is big enough. It is important to notice that the constants arising within the error estimates are independent of the physical and discretization parameters, what makes the proposed iterative scheme a parameter-robust solver.

From the values of  $\gamma$  satisfying the convergence property in Theorem 4.1, however, we want

to choose one that improves the convergence of the initially derived algorithm (32)-(33). In order to do that, we deeply analyze the application of the iterative algorithm to the one-dimensional Terzaghi problem in (24). With this purpose, we consider the reduction of the norm of the residual below  $10^{-8}$  as the stopping criterion and we analyze the number of iterations needed for convergence of the proposed scheme for different values of parameter  $\gamma$ . For illustrative purposes and without restricting the generality of the analysis, we prescribe the following values for the physical parameters of the problem as follows: the hydraulic conductivity is  $K = 10^{-10}$ ,  $\lambda + 2\mu = 1$ ,  $\alpha = 1$ , and the mesh size is chosen as  $h = 1/32$ . Notice that these values are representative and do not affect the generality of the conclusions. Then, in Figure 5, we display the number of iterations needed for convergence when the proposed iterative coupling scheme is used for solving Terzaghi problem with the stabilized P1-P1 discretization derived in (25)-(26), for different values of parameter  $\gamma$ . It is observed that only two iterations are needed when  $\gamma = 2/3$ ,

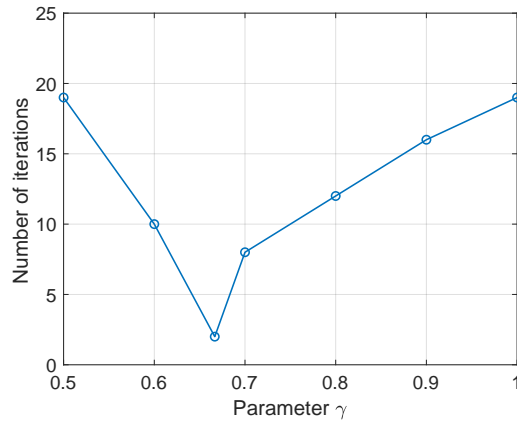


Figure 5: Number of iterations of the iterative coupling method for different values of  $\gamma$ , when the stabilized P1-P1 discretization of Terzaghi's problem is considered.

which seems to be the optimal value, since other values of  $\gamma$  provide a higher number of iterations. Next, based on this numerical insights, we derive and rigorously prove the following result for the one-dimensional case we are dealing with.

**Theorem 4.2.** *Iterative method (34)-(35) with parameter  $\gamma = \frac{2}{3}$  converges in two iterations for the stabilized P1-P1 discretization of Terzaghi's problem.*

*Proof.* From the block form of the fully-discrete stabilized scheme given in (28), we can write

the matrix block form including parameter  $\gamma$  as follows:

$$\mathcal{A}_{stab} = \begin{pmatrix} A & G \\ D & \tau A_p + \beta^{-1}M + L(M_l - M) \end{pmatrix} = \begin{pmatrix} A & G \\ D & \underbrace{\tau A_p + \beta^{-1}M + \gamma LM_l - LM - (\gamma - 1)LM_l}_C \end{pmatrix}$$

Considering the one dimensional Terzaghi problem makes that we can explicitly calculate the Schur complement,  $S_p$ , for the considered stabilized P1-P1 discretization. In particular, it is easily derived that

$$S_p - C = -DA^{-1}G = \frac{\alpha^2}{\lambda + 2\mu} \left( \frac{3}{2}M - \frac{1}{2}M_l \right) = \underbrace{\frac{3\alpha^2}{2(\lambda + 2\mu)}}_L M + \underbrace{\left( -\frac{1}{2} \frac{\alpha^2}{\lambda + 2\mu} \right)}_{(\gamma-1)L} M_l = LM + (\gamma - 1)LM_l,$$

where in the last equality we have used that  $L = \frac{3\alpha^2}{2(\lambda + 2\mu)}$  and  $\gamma = \frac{2}{3}$ . By using the equality that we just obtained, we can write the splitting corresponding to the iterative method (34)-(35) given in (36) in the following way:

$$\begin{aligned} \mathcal{A}_{stab} &= \begin{pmatrix} A & G \\ 0 & \tau A_p + \beta^{-1}M + \gamma LM_l \end{pmatrix} - \begin{pmatrix} 0 & 0 \\ -D & LM + (\gamma - 1)LM_l \end{pmatrix} \\ (42) \quad &= \begin{pmatrix} A & G \\ D & C \end{pmatrix} = \begin{pmatrix} A & G \\ 0 & S_p \end{pmatrix} - \begin{pmatrix} 0 & 0 \\ -D & S_p - C \end{pmatrix}, \end{aligned}$$

If considering the iteration matrix  $\mathcal{S}$  corresponding to splitting (42), that is.,

$$\mathcal{S} = \mathcal{I} - \mathcal{B}\mathcal{A}_{stab}, \text{ where } \mathcal{B} = \begin{pmatrix} A & G \\ 0 & S_p \end{pmatrix}^{-1},$$

we can write that

$$\begin{aligned} \mathcal{S}^2 &= (\mathcal{I} - \mathcal{B}\mathcal{A}_{stab})(\mathcal{I} - \mathcal{B}\mathcal{A}_{stab}) = \mathcal{B}(\mathcal{I} - \mathcal{A}_{stab}\mathcal{B})(\mathcal{I} - \mathcal{A}_{stab}\mathcal{B})\mathcal{B}^{-1} \\ (43) \quad &= \mathcal{B}(\mathcal{I} - \mathcal{A}_{stab}\mathcal{B})^2\mathcal{B}^{-1}. \end{aligned}$$

We now consider the block- $\mathcal{LU}$  factorization of  $\mathcal{A}_{stab}$ , i.e.,

$$\mathcal{A}_{stab} = \begin{pmatrix} A & G \\ D & C \end{pmatrix} = \begin{pmatrix} I & 0 \\ DA^{-1} & I \end{pmatrix} \begin{pmatrix} A & G \\ 0 & S_p \end{pmatrix} =: \mathcal{LU}.$$

Since  $\mathcal{B} = \mathcal{U}^{-1}$ , then  $\mathcal{I} - \mathcal{A}_{stab}\mathcal{B} = \mathcal{I} - \mathcal{LU}\mathcal{U}^{-1} = \mathcal{I} - \mathcal{L} = \begin{pmatrix} 0 & 0 \\ -DA^{-1} & 0 \end{pmatrix}$ . This implies that  $(\mathcal{I} - \mathcal{A}_{stab}\mathcal{B})^2 = 0$  and, consequently, from (43) we obtain that  $\mathcal{S}^2 = 0$ , what means that the iterative coupling scheme converges in only two iterations.  $\square$

Summarizing, we have seen that the proposed iterative coupling method (34)-(35) is optimal in the one-dimensional case when  $\gamma = 2/3$  is assumed, since only two iterations are enough for the solution of the complex coupled Biot's problem. The question now is how it behaves for higher dimensional problems. In order to analyze that, we consider here the two-dimensional benchmark problem of Barry & Mercer which has been previously introduced in Example 3.1.3. An example of application for a three-dimensional problem was also studied in [62].

#### 4.1.1 NUMERICAL EXPERIMENT. BARRY & MERCER PROBLEM

In order to apply the proposed iterative coupling method in higher dimensions, we fix the value of parameter  $\gamma$  which was demonstrated to be optimal in the one-dimensional case. Of course, this does not mean that it is optimal for the two-dimensional case, but we will show that this choice provides almost optimal results in all the tests carried out.

In order to numerically illustrate the suitability of the choice of  $\gamma$ , we consider two different test cases with different values of the Poisson ratio  $\nu$  and hydraulic conductivity  $K$  and different grid sizes, and we analyze the number of iterations of the proposed scheme for different values of parameter  $\gamma$ . This can be observed in Figure 6, where we fix  $h = 1/32$  and consider two values of hydraulic conductivity:  $K = 10^{-10}$  and  $K = 10^{-2}$ , and two values for the Poisson ratio  $\nu = 0.2$  and  $\nu = 0.4$ . We observe from the figures that the choice of  $\gamma$  has little influence when  $K$  is large, whereas for small values of  $K$  selecting an appropriate value of parameter  $\gamma$  becomes crucial. Moreover, unlike in the one-dimensional setting, here the choice of  $\gamma = 2/3$  is not optimal for both values of  $\nu$ : it performs optimally for  $\nu = 0.4$  but not for  $\nu = 0.2$ . Nevertheless, choosing  $\gamma = 2/3$  still yields very good, almost optimal, results in both cases, as illustrated in the two pictures.

Next, we analyze the parameter-robustness of the proposed iterative coupling algorithm (34)-(35). With this purpose, in Table 1, we show the number of iterations of the method for

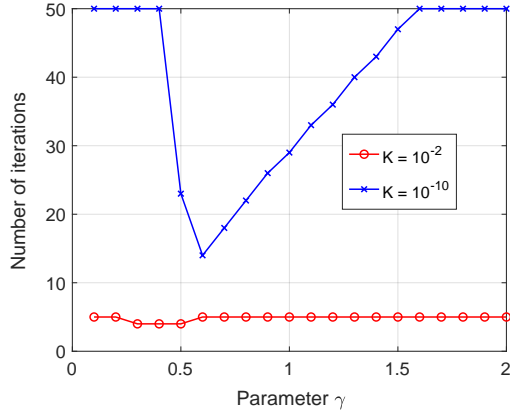
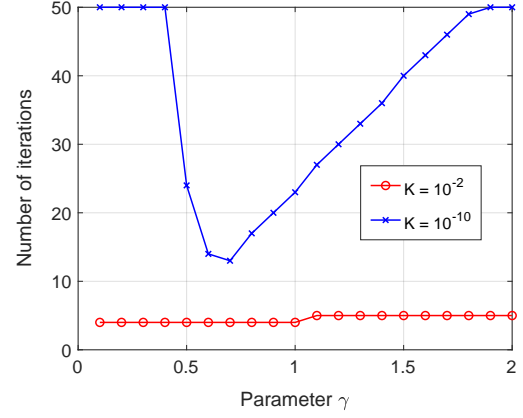
(a)  $\nu = 0.2$ (b)  $\nu = 0.4$ 

Figure 6: Number of iterations of the iterative coupling scheme for different values of  $\gamma$  for the Barry & Mercer's problem.

several values of the hydraulic conductivity  $K$  and the mesh size  $h$ . The stopping criterion considered to obtain the results is fixed as  $\|\delta p_h^{n,i}\| + \|\delta \mathbf{u}_h^{n,i}\| \leq 10^{-8}$  where  $\delta p_h^{n,i} = p_h^{n,i} - p_h^{n,i-1}$  and  $\delta \mathbf{u}_h^{n,i} = \mathbf{u}_h^{n,i} - \mathbf{u}_h^{n,i-1}$  denote the difference between two successive approximations for displacements and for pressure, respectively. From the table, we can observe that the number of iterations stays relatively stable for all the different values of  $K$  and  $h$ .

$K$	$h = 1/16$	$h = 1/32$	$h = 1/64$	$h = 1/128$
$10^{-2}$	4	4	4	4
$10^{-4}$	6	6	6	6
$10^{-6}$	11	11	11	11
$10^{-8}$	15	15	15	15
$10^{-10}$	11	11	12	12
$10^{-12}$	6	7	7	8

Table 1: Number of iterations of Algorithm (34)-(35) with  $\gamma = 2/3$ , considering  $E = 10^5$ ,  $\nu = 0.4$ , different mesh sizes  $h$  and different values of the hydraulic conductivity  $K$ .

We repeat the same numerical test but fixing the value of the hydraulic conductivity to  $K = 10^{-10}$  and varying the value of the Poisson ratio in a range from 0.1 to 0.49. Different grid sizes are considered again and the number of iterations of algorithm (34)-(35) is shown in Table 2. Again, the method shows a robust performance with respect to the considered parameters.

$\nu$	$h = 1/16$	$h = 1/32$	$h = 1/64$	$h = 1/128$
0.1	18	20	21	22
0.2	16	17	18	19
0.3	13	14	15	16
0.4	11	11	12	12
0.49	12	11	9	8

Table 2: Number of iterations of Algorithm (34)-(35) with  $\gamma = 2/3$ , considering  $E = 10^5$ ,  $K = 10^{-10}$ , different mesh sizes  $h$  and different values of Poisson ratio  $\nu$ .

**Remark 4.3** (More general fluid regimes). *In a more general case in which the storage coefficient  $\beta^{-1}$  is not close to zero, it is not possible to find a parameter  $\gamma$  in (36) that provides an optimal iterative coupling method that converges in two iterations for the one-dimensional Terzaghi problem. We can include, however, a second parameter into the iterative coupling method in order to obtain similar results to the presented in the previous case. We then consider two parameters  $\gamma_1, \gamma_2 > 0$ , and if  $\mathbf{u}_h^{n,0} = \mathbf{u}_h^{n-1}$  and  $p_h^{n,0} = p_h^{n-1}$  are the initial guesses of the iterative scheme at time  $t_n$ , the new improved algorithm provides a sequence of approximations  $(\mathbf{u}_h^{n,i}, p_h^{n,i}), i \geq 1$  as follows:*

**Step 1:** Given  $(\mathbf{u}_h^{n,i-1}, p_h^{n,i-1}) \in \mathbf{V}_h \times Q_h$ , find  $p_h^{n,i} \in Q_h$  such that:

$$\begin{aligned}
& \frac{1}{\beta} \left( \frac{p_h^{n,i} - p_h^{n-1}}{\tau}, q_h \right) + \gamma_1 L \left( \frac{p_h^{n,i} - p_h^{n-1}}{\tau}, q_h \right)_0 - \gamma_2 L \left( \frac{p_h^{n,i} - p_h^{n-1}}{\tau}, q_h \right) + a_p(p_h^{n,i}, q_h) = \\
& \quad + (1 - \gamma_2) L \left( \frac{p_h^{n,i-1} - p_h^{n-1}}{\tau}, q_h \right) + (\gamma_1 - 1) L \left( \frac{p_h^{n,i-1} - p_h^{n-1}}{\tau}, q_h \right)_0 \\
(44) \quad & \quad - \alpha \left( \operatorname{div} \frac{\mathbf{u}_h^{n,i-1} - \mathbf{u}_h^{n-1}}{\tau}, q_h \right) + (g_h^n, q_h), \quad \forall q_h \in Q_h,
\end{aligned}$$

**Step 2:** Given  $p_h^{n,i} \in Q_h$ , find  $\mathbf{u}_h^{n,i} \in \mathbf{V}_h$  such that

$$(45) \quad a(\mathbf{u}_h^{n,i}, \mathbf{v}_h) = \alpha(p_h^{n,i}, \operatorname{div} \mathbf{v}_h) + (\mathbf{f}_h^n, \mathbf{v}_h), \quad \forall \mathbf{v}_h \in \mathbf{V}_h.$$

Similarly as previously done in Theorem 4.1, we can prove the convergence of the iterative coupling method (44) -(45), which results to be robust with respect to the physical and discretization parameters of the problem.

**Theorem 4.4.** *The iterative method given in (44)-(45) is convergent for any parameters  $\gamma_1 \in (2/3, 2]$ ,  $\gamma_1 > \gamma_2 \geq 0$ , such that  $(\gamma_1 - \gamma_2)L = \omega \frac{\alpha^2}{(\lambda+2\mu/d)} \geq \frac{\alpha^2}{(\lambda+2\mu/d)}$ , i.e.,  $\omega \geq 1$ . Additionally,*

$$(46) \quad \|e_p^i\|^2 + \frac{|1 - \gamma_1|}{\gamma_1 - \gamma_2} \|e_p^i\|_Z^2 \leq \frac{1}{1 + \frac{\eta^2}{\omega(1+2\theta^*)}} \left( \|e_p^{i-1}\|^2 + \frac{|1 - \gamma_1|}{\gamma_1 - \gamma_2} \|e_p^{i-1}\|_Z^2 \right),$$

where  $\theta^* \geq \frac{\epsilon^2 C_2 \gamma_1}{4\omega(\gamma_1 - |1 - \gamma_1|)}$  is a root of the quadratic equation (38) (with  $\gamma$  replaced by  $\gamma_1$ ). Here,  $\eta > 0$  is the constant appearing in the weak inf-sup condition (31) and  $C_2$  is the constant for the upper bound of the spectral equivalence condition (29).

Finally, in order to optimize the convergence of algorithm (44)-(45), we can analyze the one-dimensional problem to obtain the optimal values for  $\gamma_1$  and  $\gamma_2$ .

**Theorem 4.5.** *Iterative method (44)-(45) with parameters  $\gamma_1 = 1 - \frac{1}{2L(\lambda + 2\mu)}$ , and  $\gamma_2 = 1 - \frac{3}{2L(\lambda + 2\mu)}$ , with  $L$  as in (27) converges in two iterations for the stabilized P1-P1 discretization of Terzaghi's problem.*

The proofs of Theorems 4.4 and 4.5 can be found in [62], as well as more details for this general case.

## 4.2 Non-iterative coupling method

The explicit coupling approach considered here is based on the idea behind the so-called explicit fixed-stress split scheme, which is widely used in practice (see for example [54, 25, 24] and the references therein). In such a decoupled method, the flow problem (12) is solved first with time-lagging the displacement term followed by the mechanic problem (11). As well as in the iterative coupling fixed-stress split method, a stabilization term should be added in the flow equation for convergence reasons. Here, by considering the stabilized scheme in (25)-(26), we can construct a similar decoupled algorithm avoiding the need to add a different parameter to stabilize the solution algorithm. We want to emphasize that the proposed non-iterative coupling method for the stabilized P1-P1 discretization provides one of the simplest numerical scheme for addressing the coupled multiphysics Biot's problem.

In order to define the explicit coupling algorithm, we must slightly change the time-discretization of the stabilized problem. In particular, we now consider the backward Euler method to discretize the terms corresponding to  $\frac{1}{\beta}(\partial_t p_h, q_h)$  and  $L(\partial_t p_h, q_h)_0$  and a forward Euler method for the

terms  $L(\partial_t p_h, q_h)$  and  $\alpha(\operatorname{div} \partial_t \mathbf{u}_h, q_h)$ . More concretely, if we again consider a uniform partition of the time interval  $(0, T_f]$ ,  $t_n = n\tau$ ,  $n = 0, \dots, N$ , with time-step  $\tau = T_f/N$ , and let  $(\mathbf{u}_h^n, p_h^n)$  be the approximation of  $(\mathbf{u}_h(t), p_h(t))$  at time level  $t_n$ , we can write the fully discrete stabilized scheme as follows:

$$(47) \quad a(\mathbf{u}_h^{n+1}, \mathbf{v}_h) - \alpha(p_h^{n+1}, \operatorname{div} \mathbf{v}_h) = (\mathbf{f}_h^{n+1}, \mathbf{v}_h), \quad \forall \mathbf{v}_h \in \mathbf{V}_h,$$

$$(48) \quad \frac{1}{\beta}(\bar{\partial}_t^f p_h^n, q_h) + \alpha(\operatorname{div} \bar{\partial}_t^b \mathbf{u}_h^n, q_h) + a_p(p_h^{n+1}, q_h) + L(\bar{\partial}_t^f p_h^n, q_h)_0 - L(\bar{\partial}_t^b p_h^n, q_h) \\ = (g_h^{n+1}, q_h), \quad \forall q_h \in Q_h,$$

where  $\bar{\partial}_t^f p_h^n := (p_h^{n+1} - p_h^n)/\tau$ ,  $\bar{\partial}_t^b p_h^n := (p_h^n - p_h^{n-1})/\tau$  and  $\bar{\partial}_t^b \mathbf{u}_h^n := (\mathbf{u}_h^n - \mathbf{u}_h^{n-1})/\tau$ .

Notice that the resulting fully discrete problem is an explicit coupling approach in which on each time level the flow problem is solved first followed for the mechanic problem, and therefore, there is no coupling between both problems anymore, as shown in the following algorithm:

**For**  $n = 1, 2, \dots, N - 1$

**Step 1:** Given  $(\mathbf{u}_h^n, \mathbf{u}_h^{n-1}, p_h^n, p_h^{n-1}) \in \mathbf{V}_h \times \mathbf{V}_h \times Q_h \times Q_h$ , find  $p_h^{n+1} \in Q_h$  such that:

$$(49) \quad \frac{1}{\beta} \left( \frac{p_h^{n+1} - p_h^n}{\tau}, q_h \right) + L \left( \frac{p_h^{n+1} - p_h^n}{\tau}, q_h \right)_0 + a_p(p_h^{n+1}, q_h) = -\alpha \left( \operatorname{div} \frac{\mathbf{u}_h^n - \mathbf{u}_h^{n-1}}{\tau}, q_h \right) + \\ + L \left( \frac{p_h^n - p_h^{n-1}}{\tau}, q_h \right) + (g_h^{n+1}, q_h), \quad \forall q_h \in Q_h,$$

**Step 2:** Given  $p_h^{n+1} \in Q_h$ , find  $\mathbf{u}_h^{n+1} \in \mathbf{V}_h$  such that

$$(50) \quad a(\mathbf{u}_h^{n+1}, \mathbf{v}_h) = \alpha(p_h^{n+1}, \operatorname{div} \mathbf{v}_h) + (\mathbf{f}_h^{n+1}, \mathbf{v}_h), \quad \forall \mathbf{v}_h \in \mathbf{V}_h.$$

Regarding the initial conditions to apply algorithm (49)-(50), previously we need to obtain  $p_h^1$ , and therefore a fully implicit scheme is used to obtain the solution at the first time level  $(\mathbf{u}_h^1, p_h^1)$ .

In particular, the following problem is solved:

$$(51) \quad a(\mathbf{u}_h^1, \mathbf{v}_h) - \alpha(p_h^1, \operatorname{div} \mathbf{v}_h) = (\mathbf{f}_h^1, \mathbf{v}_h), \quad \forall \mathbf{v}_h \in \mathbf{V}_h,$$

$$\frac{1}{\beta} \left( \frac{p_h^1 - p_h^0}{\tau}, q_h \right) + L \left( \frac{p_h^1 - p_h^0}{\tau}, q_h \right)_0 + \alpha \left( \operatorname{div} \frac{\mathbf{u}_h^1 - \mathbf{u}_h^0}{\tau}, q_h \right) + a_p(p_h^1, q_h)$$

$$(52) \quad -L \left( \frac{p_h^1 - p_h^0}{\tau}, q_h \right) = (g_h^1, q_h), \quad \forall q_h \in Q_h.$$

Next, we demonstrate that the explicit coupling scheme (49)-(50) is optimally convergent. Let us define the errors at  $t = t_n$  as follows  $e_{\mathbf{u}}^n = \mathbf{u}(t_n) - \mathbf{u}_h^n$  and  $e_p^n = p(t_n) - p_h^n$ .

**Theorem 4.6.** *Let  $\mathbf{u}(t)$  and  $p(t)$  be the solutions of (17) and (18), and  $\mathbf{u}_h^n$  and  $p_h^n$  be the solutions obtained by Algorithm (49)-(50). If  $L = \omega \frac{\alpha^2}{\lambda + 2\mu/d}$ ,  $\omega \geq 1$ , then the following error estimates hold,*

$$(53) \quad \begin{aligned} & \|\mathbf{u}(t_n) - \mathbf{u}_h^n\|_A + \|p(t_n) - p_h^n\| \\ & \leq C \left( \|e_{\mathbf{u}}^0\|_A + \|e_p^0\|_{A_p} \right) + Ch \left( |u(t_0)|_2 + |p(t_0)|_1 + |p(t_0)|_2 + |u(t_n)|_2 + |p(t_n)|_1 \right) \\ & \quad + C\tau \left[ \left( \int_{t_0}^{t_{n+1}} \|\partial_{tt} p(s)\|_2^2 ds \right)^{\frac{1}{2}} + \left( \int_{t_0}^{t_{n+1}} \|\partial_{tt} \mathbf{u}(s)\|_1^2 ds \right)^{\frac{1}{2}} \right] \\ & \quad + Ch \left[ \left( \int_{t_0}^{t_{n+1}} h^2 |\partial_t p(s)|_2^2 ds \right)^{\frac{1}{2}} + \left( \int_{t_0}^{t_{n+1}} |\partial_t \mathbf{u}|_2^2 + |\partial_t p|_1^2 ds \right)^{\frac{1}{2}} + \left( \tau \sum_{j=1}^n |\partial_t p(t_{j+1})|_1^2 \right)^{\frac{1}{2}} \right] \\ & \quad + Ch\tau \left( \int_{t_0}^{t_{n+1}} |\partial_{tt} p(s)|_1^2 ds \right)^{\frac{1}{2}}. \end{aligned}$$

*Proof.* Because of the technical and lengthy nature of the proof, we do not include it here. A detailed proof is provided in [40].  $\square$

#### 4.2.1 NUMERICAL EXPERIMENT. 2D PROBLEM WITH A MANUFACTURED SOLUTION

Now, we present some numerical results in two-dimensions to validate our theoretical estimates. We consider the unit square as domain, i.e.  $\Omega = (0, 1) \times (0, 1) \subset \mathbb{R}^2$ , and we take the source terms, initial and Dirichlet boundary conditions such that the exact solution of problem (11)-(12) is as follows:

$$(54) \quad u(x, y, t) = v(x, y, t) = p(x, y, t) = t^3 \sin(\pi x) \sin(\pi y),$$

The following physical parameters are considered:  $\lambda = 1, \mu = 2, \alpha = 1, \beta = 100, K = 1$ , and a final time of  $T_f = 1$  is fixed. Then, we apply the non-iterative coupling algorithm (49)-(50) to solve the stabilized P1-P1 discrete scheme of Biot's model.

We compute the errors between the exact solution and the numerical solution of the pressure obtained by applying algorithm (49)-(50), i.e.  $\|u - u_h^{dec}\|_\infty$ , and also we compute the corresponding errors when the problem is solved with a fully-implicit method (or an iterative coupling scheme, since the numerical solution is the same) i.e.  $\|u - u_h^{fully}\|_\infty$ , for comparison. Such errors are calculated in the maximum norm, and are shown in Table 3, where also the convergence rates in the case of the errors for the decoupled scheme are displayed. We observe that by refining the time step  $\tau$  and mesh size  $h$  appropriately, the errors decrease with a rate of approximately 2, indicating first order of convergence, as expected from the theoretical analysis. Moreover, the obtained errors with the fully-implicit method and the explicit coupling algorithm are both small with similar order of magnitude.

$h$	$\tau$	$\ u - u_h^{fully}\ _\infty$	$\ u - u_h^{dec}\ _\infty$	rate
1/100	1/40	$2.7646e - 03$	$7.7593e - 03$	
1/200	1/80	$1.2669e - 03$	$3.8973e - 03$	1.99
1/400	1/160	$6.0461e - 04$	$1.9528e - 03$	1.99
1/800	1/320	$2.9508e - 04$	$9.7740e - 04$	2.00

Table 3: Errors in maximum norm between the exact solution and the numerical solution obtained from the explicit coupling algorithm (49)-(50)  $\|u - u_h^{dec}\|_\infty$  and also from the application of a fully-implicit method  $\|u - u_h^{fully}\|_\infty$ , together with the corresponding convergence rate for the first case, for different values of the time and spatial discretization parameters  $\tau$  and  $h$ , respectively.

## 5 Conclusions

In this work, we have addressed the two central challenges arising in the numerical simulation of Biot's model: the design of a stable discretization strategy capable of producing solutions free from nonphysical oscillations, and the development of an efficient and robust solver for the resulting large linear systems. To this end, we proposed a novel stabilization technique that offers several advantages over existing approaches. First, the method does not depend on the mesh size  $h$  or on any other discretization parameters. Second, it is derived for arbitrary values of the storage coefficient, ensuring broad applicability. Third, the particular structure of the stabilization naturally leads to coupling schemes between the fluid and mechanics subproblems (iterative and

non-iterative) that converge without requiring any additional stabilization terms. As a consequence, we obtain parameter-robust decoupled solvers for the fully coupled system. Furthermore, the proposed iterative coupling algorithm can be tuned to achieve optimal convergence behavior in one-dimensional settings and nearly optimal performance in two and three dimensions. The combination of the stabilized finite element scheme, based on simple piecewise linear functions for both displacement and pressure variables, and the resulting decoupled solvers thus provides a simple, efficient, practical and reliable computational framework for the simulation of Biot’s model.

## Acknowledgments

I would like to thank all the members of ‘Real Academia de Ciencias Exactas, Físicas, Químicas y Naturales de Zaragoza’, specially the members of the ‘Sección de Exactas’ for nominating me for the Academy award. It is a great honor for me to receive such a great distinction. I would also like to thank Prof. Francisco J. Gaspar and Prof. Francisco J. Lisbona for introducing me to the Biot’s model and the fascinating world of poromechanics and for their support along my whole research career. Last but not least, I would like to thank my collaborators that contributed to the results presented in this work: Francisco J. Gaspar and Álvaro Pé de la Riva (University of Zaragoza), Xiaozhe Hu and James Adler (Tufts University, USA) and Ludmil Zikatanov (The Pennsylvania State University, USA). This work is partially supported by the Diputación General de Aragón, Spain (Grupo de referencia APEDIF, ref. E24\_23R) and by the Spanish Grant PID2022-140108NB-I00 funded by MCIN/AEI/10.13039/501100011033 and by “ERDF A way of making Europe”, and by the “European Union NextGenerationEU/PRTR”.

## References

- [1] Y. Abousleiman, A. H.-D. Cheng, L. Cui, E. Detournay, and J.-C. Roegiers. Mandel’s problem revisited. *Géotechnique*, 46(2):187–195, 1996.
- [2] J. H. Adler, F. J. Gaspar, X. Hu, P. Ohm, C. Rodrigo, and L. T. Zikatanov. Robust preconditioners for a new stabilized discretization of the poroelastic equations. *SIAM Journal on Scientific Computing*, 42(3):B761–B791, 2020.
- [3] James H. Adler, Francisco J. Gaspar, Xiaozhe Hu, Carmen Rodrigo, and Ludmil T. Zikatanov. Robust block preconditioners for Biot’s model. In Petter E. Bjørstad, Susanne C. Brenner, Lawrence Halpern, Hyea Hyun Kim, Ralf Kornhuber, Talal Rahman, and Olof B. Widlund, editors, *Domain*

*Decomposition Methods in Science and Engineering XXIV*, pages 3–16, Cham, 2018. Springer International Publishing.

- [4] James H. Adler, Yunhui He, Xiaozhe Hu, Scott MacLachlan, and Peter Ohm. Monolithic multigrid for a reduced-quadrature discretization of poroelasticity. *SIAM Journal on Scientific Computing*, 45(3):S54–S81, 2023.
- [5] G. Aguilar, F. Gaspar, F. Lisbona, and C. Rodrigo. Numerical stabilization of Biot’s consolidation model by a perturbation on the flow equation. *International Journal for Numerical Methods in Engineering*, 75(11):1282–1300, 2008.
- [6] T. Almani, K. Kumar, G. Singh, and M.F. Wheeler. Stability of multirate explicit coupling of geomechanics with flow in a poroelastic medium. *Computers & Mathematics with Applications*, 78(8):2682–2699, 2019.
- [7] D.N. Arnold, F. Brezzi, and M. Fortin. A stable finite element for the Stokes equations. *Calcolo*, 21(4):337–344, 1985.
- [8] Khalid Aziz and Antonín Settari. *Petroleum Reservoir Simulation*. Society of Petroleum Engineers, 1979.
- [9] S. I. Barry and G. N. Mercer. Exact solutions for two-dimensional time-dependent flow and deformation within a poroelastic medium. *Journal of Applied Mechanics*, 66(2):536–540, 10 1999.
- [10] Mario Bebendorf. A note on the Poincaré inequality for convex domains. *Zeitschrift für Analysis und ihre Anwendungen*, 22(4):751–756, 2003.
- [11] F. Ben-Hatira, K. Saidane, and A. Mrabet. A finite element modeling of the human lumbar unit including the spinal cord. *Journal of Biomedical Science and Engineering*, 5:146–152, 2012.
- [12] Luca Bergamaschi, Massimiliano Ferronato, and Giuseppe Gambolati. Novel preconditioners for the iterative solution to FE-discretized coupled consolidation equations. *Computer Methods in Applied Mechanics and Engineering*, 196(25):2647–2656, 2007.
- [13] Lorenz Berger, Rafel Bordas, David Kay, and Simon Tavener. Stabilized lowest-order finite element approximation for linear three-field poroelasticity. *SIAM Journal on Scientific Computing*, 37(5):A2222–A2245, 2015.
- [14] Maurice A. Biot. General theory of three-dimensional consolidation. *Journal of Applied Physics*, 12(2):155–164, 1941.

- [15] Maurice A. Biot. Theory of elasticity and consolidation for a porous anisotropic solid. *Journal of Applied Physics*, 26(2):182–185, 1955.
- [16] Manuel Borregales, Kundan Kumar, Florin Adrian Radu, Carmen Rodrigo, and Francisco José Gaspar. A partially parallel-in-time fixed-stress splitting method for Biot’s consolidation model. *Computers & Mathematics with Applications*, 77(6):1466 – 1478, 2019. 7th International Conference on Advanced Computational Methods in Engineering (ACOMEN 2017).
- [17] Jakub Wiktor Both, Manuel Borregales, Jan Martin Nordbotten, Kundan Kumar, and Florin Adrian Radu. Robust fixed stress splitting for Biot’s equations in heterogeneous media. *Applied Mathematics Letters*, 68:101 – 108, 2017.
- [18] Trygve Bærland, Jeonghun J. Lee, Kent-Andre Mardal, and Ragnar Winther. Weakly imposed symmetry and robust preconditioners for Biot’s consolidation model. *Computational Methods in Applied Mathematics*, 17(3):377–396, 2017.
- [19] Mingchao Cai, Huipeng Gu, Jingzhi Li, and Mo Mu. Some optimally convergent algorithms for decoupling the computation of Biot’s model. *Journal of Scientific Computing*, 97(2):48, 2023.
- [20] N. Castelletto, J. A. White, and H. A. Tchelepi. Accuracy and convergence properties of the fixed-stress iterative solution of two-way coupled poromechanics. *International Journal for Numerical and Analytical Methods in Geomechanics*, 39(14):1593–1618, 2015.
- [21] Nabil Chaabane and Béatrice Rivière. A splitting-based finite element method for the Biot poroelasticity system. *Computers & Mathematics with Applications*, 75(7):2328–2337, 2018.
- [22] Shuangshuang Chen, Qingguo Hong, Jinchao Xu, and Kai Yang. Robust block preconditioners for poroelasticity. *Computer Methods in Applied Mechanics and Engineering*, 369:113229, 2020.
- [23] Zhangxin Chen, Guanren Huan, and Yuanle Ma. *Computational Methods for Multiphase Flows in Porous Media*. Society for Industrial and Applied Mathematics, 2006.
- [24] R. H. Dean, X. Gai, C. M. Stone, and S. E. Minkoff. A comparison of techniques for coupling porous flow and geomechanics. *SPE Journal*, 11(01):132–140, 03 2006.
- [25] Dennis Denney. Coupled reservoir simulation: Management of production- induced stress sensitivity. *Journal of Petroleum Technology*, 53(04):80–81, 04 2001.
- [26] M. Favino, A. Grillo, and R. Krause. A stability condition for the numerical simulation of poroelastic systems. In Christian Hellmich, Bernhard Pichler, and Dietmar Adam, editors, *Poromechanics V: Proceedings of the Fifth Biot Conference on Poromechanics*, pages 919–928, 2013.

- [27] Massimiliano Ferronato, Luca Bergamaschi, and Giuseppe Gambolati. Performance and robustness of block constraint preconditioners in finite element coupled consolidation problems. *International Journal for Numerical Methods in Engineering*, 81(3):381–402, 2010.
- [28] Massimiliano Ferronato, Nicola Castelletto, and Giuseppe Gambolati. A fully coupled 3-d mixed finite element model of Biot consolidation. *Journal of Computational Physics*, 229(12):4813–4830, 2010.
- [29] X. Gai. *A coupled geomechanics and reservoir flow model on parallel computers*. PhD thesis, The University of Texas at Austin, Austin, Texas, 2004.
- [30] X. Gai, S. Sun, M. F. Wheeler, and H. Klie. A time stepping scheme for coupled reservoir flow and geomechanics on nonmatching grids. volume SPE Annual Technical Conference and Exhibition of *SPE Annual Technical Conference and Exhibition*, pages SPE–97054–MS, October 2005.
- [31] F. J. Gaspar, J. L. Gracia, F. J. Lisbona, and C. W. Oosterlee. Distributive smoothers in multigrid for problems with dominating grad-div operators. *Numer. Linear Algebra Appl.*, 15(8):661–683, 2008.
- [32] F. J. Gaspar, F. J. Lisbona, C. W. Oosterlee, and R. Wienands. A systematic comparison of coupled and distributive smoothing in multigrid for the poroelasticity system. *Numerical Linear Algebra with Applications*, 11(2-3):93–113, 2004.
- [33] F. J. Gaspar, F. J. Lisbona, and P. N. Vabishchevich. A finite difference analysis of Biot’s consolidation model. *Appl. Numer. Math.*, 44(4):487–506, 2003.
- [34] F. J. Gaspar, F. J. Lisbona, and P. N. Vabishchevich. Staggered grid discretizations for the quasi-static Biot’s consolidation problem. *Appl. Numer. Math.*, 56(6):888–898, 2006.
- [35] Francisco J. Gaspar and Carmen Rodrigo. On the fixed-stress split scheme as smoother in multigrid methods for coupling flow and geomechanics. *Computer Methods in Applied Mechanics and Engineering*, 326:526 – 540, 2017.
- [36] Joachim Berdal Haga, Harald Osnes, and Hans Petter Langtangen. Efficient block preconditioners for the coupled equations of pressure and deformation in highly discontinuous media. *International Journal for Numerical and Analytical Methods in Geomechanics*, 35(13):1466–1482, 2011.
- [37] Joachim Berdal Haga, Harald Osnes, and Hans Petter Langtangen. On the causes of pressure oscillations in low-permeable and low-compressible porous media. *International Journal for Numerical and Analytical Methods in Geomechanics*, 36(12):1507–1522, 2012.

- [38] Q. Hong and J. Kraus. Parameter-robust stability of classical three-field formulation of Biot’s consolidation model. *Elec. Transact. Numer. Anal.*, 48:202–226, 2018.
- [39] Qingguo Hong, Johannes Kraus, Maria Lybery, and Fadi Philo. Conservative discretizations and parameter-robust preconditioners for Biot and multiple-network flux-based poroelasticity models. *Numerical Linear Algebra with Applications*, 26(4):e2242, 2019.
- [40] Xiaozhe Hu, Francisco J. Gaspar, and Carmen Rodrigo. Convergence analysis for non-iterative sequential schemes for Biot’s model. *Submitted for publication*, 2025.
- [41] Xiaozhe Hu, Carmen Rodrigo, Francisco J. Gaspar, and Ludmil T. Zikatanov. A nonconforming finite element method for the Biot’s consolidation model in poroelasticity. *Journal of Computational and Applied Mathematics*, 310:143 – 154, 2017.
- [42] J. Kim, H.A. Tchelepi, and R. Juanes. Stability and convergence of sequential methods for coupled flow and geomechanics: Drained and undrained splits. *Computer Methods in Applied Mechanics and Engineering*, 200(23):2094–2116, 2011.
- [43] J. Kim, H.A. Tchelepi, and R. Juanes. Stability and convergence of sequential methods for coupled flow and geomechanics: Fixed-stress and fixed-strain splits. *Computer Methods in Applied Mechanics and Engineering*, 200(13):1591–1606, 2011.
- [44] J.. Kim, H.A.. A. Tchelepi, and R.. Juanes. Stability, Accuracy, and Efficiency of Sequential Methods for Coupled Flow and Geomechanics. *SPE Journal*, 16(02):249–262, 01 2011.
- [45] Johannes Korsawe and Gerhard Starke. A least-squares mixed finite element method for Biot’s consolidation problem in porous media. *SIAM Journal on Numerical Analysis*, 43(1):318–339, 2005.
- [46] Jeonghun J. Lee. Robust three-field finite element methods for Biot’s consolidation model in poroelasticity. *BIT Numerical Mathematics*, 58:347–372, 2018.
- [47] Jeonghun J. Lee, Kent-Andre Mardal, and Ragnar Winther. Parameter-robust discretization and preconditioning of Biot’s consolidation model. *SIAM Journal on Scientific Computing*, 39(1):A1–A24, 2017.
- [48] L. J. Lee. Unconditionally stable second order convergent partitioned methods for multiple-network poroelasticity. *arXiv preprint arXiv:1901.06078*, 2019.
- [49] Sanghyun Lee and Son-Young Yi. Locking-free and locally-conservative enriched Galerkin method for poroelasticity. *Journal of Scientific Computing*, 94(1), 2023.

- [50] R.W. Lewis and B.A. Schrefler. *The Finite Element Method in the Static and Dynamic Deformation and Consolidation of Porous Media*. Wiley: New York, 1998.
- [51] P. Luo, C. Rodrigo, F. J. Gaspar, and C. W. Oosterlee. On an Uzawa smoother in multigrid for poroelasticity equations. *Numerical Linear Algebra with Applications*, 24(1):e2074–n/a, 2017. e2074 nla.2074.
- [52] J. Mandel. Consolidation des sols (Étude mathématique)\*. *Géotechnique*, 3(7):287–299, 09 1953.
- [53] Andro Mikelić and Mary F. Wheeler. Convergence of iterative coupling for coupled flow and geomechanics. *Computational Geosciences*, 17(3):455–461, 2013.
- [54] Susan E. Minkoff, C. Mike Stone, Steve Bryant, Malgorzata Peszynska, and Mary F. Wheeler. Coupled fluid flow and geomechanical deformation modeling. *Journal of Petroleum Science and Engineering*, 38(1):37–56, 2003.
- [55] Márcio A. Murad and Abimael F. D. Loula. Improved accuracy in finite element analysis of Biot’s consolidation problem. *Comput. Methods Appl. Mech. Engrg.*, 95(3):359–382, 1992.
- [56] Márcio A. Murad and Abimael F. D. Loula. On stability and convergence of finite element approximations of Biot’s consolidation problem. *Internat. J. Numer. Methods Engrg.*, 37(4):645–667, 1994.
- [57] Márcio A. Murad, Vidar Thomée, and Abimael F. D. Loula. Asymptotic behavior of semidiscrete finite-element approximations of Biot’s consolidation problem. *SIAM J. Numer. Anal.*, 33(3):1065–1083, 1996.
- [58] Jan Martin Nordbotten. Cell-centered finite volume discretizations for deformable porous media. *International Journal for Numerical Methods in Engineering*, 100(6):399–418, 2014.
- [59] Jan Martin Nordbotten. Finite volume hydromechanical simulation in porous media. *Water Resources Research*, 50(5):4379–4394, 2014.
- [60] Jan Martin Nordbotten. Stable cell-centered finite volume discretization for Biot equations. *SIAM Journal on Numerical Analysis*, 54(2):942–968, 2016.
- [61] Ricardo Oyarzúa and Ricardo Ruiz-Baier. Locking-free finite element methods for poroelasticity. *SIAM Journal on Numerical Analysis*, 54(5):2951–2973, 2016.
- [62] Álvaro Pé de la Riva, Francisco J. Gaspar, Xiaozhe Hu, James H. Adler, Carmen Rodrigo, and Ludmil T. Zikatanov. Oscillation-free numerical schemes for biot’s model and their iterative coupling solution. *SIAM Journal on Scientific Computing*, 47(3):A1809–A1834, 2025.

- [63] Phillip Joseph Phillips and Mary F. Wheeler. A coupling of mixed and continuous Galerkin finite element methods for poroelasticity I: the continuous in time case. *Computational Geosciences*, 11(2):131 – 144, 2007.
- [64] Phillip Joseph Phillips and Mary F. Wheeler. A coupling of mixed and continuous Galerkin finite element methods for poroelasticity II: the discrete-in-time case. *Computational Geosciences*, 11(2):145 – 158, 2007.
- [65] Phillip Joseph Phillips and Mary F. Wheeler. A coupling of mixed and discontinuous Galerkin finite-element methods for poroelasticity. *Computational Geosciences*, 12(4):417 – 435, 2008.
- [66] Phillip Joseph Phillips and Mary F. Wheeler. Overcoming the problem of locking in linear elasticity and poroelasticity: an heuristic approach. *Computational Geosciences*, 13(1):5–12, 2009.
- [67] K. K. Phoon, K. C. Toh, S. H. Chan, and F. H. Lee. An efficient diagonal preconditioner for finite element solution of Biot’s consolidation equations. *International Journal for Numerical Methods in Engineering*, 55(4):377–400, 2002.
- [68] R. Maier R. Altmann and B. Unger. Semi-explicit discretization schemes for weakly coupled elliptic-parabolic problems. *Mathematics of Computation*, 90:1089–1118, 2021.
- [69] C Rodrigo, FJ Gaspar, X Hu, and LT Zikatanov. Stability and monotonicity for some discretizations of the Biot’s consolidation model. *Computer Methods in Applied Mechanics and Engineering*, 298:183–204, 2016.
- [70] C. Rodrigo, X. Hu, P. Ohm, J.H. Adler, F.J. Gaspar, and L.T. Zikatanov. New stabilized discretizations for poroelasticity and the Stokes’ equations. *Computer Methods in Applied Mechanics and Engineering*, 341:467–484, 2018.
- [71] Carmen Rodrigo, Francisco J. Gaspar, James Adler, Xiaozhe Hu, Peter Ohm, and Ludmil Zikatanov. Parameter-robust preconditioners for Biot’s model. *SeMA Journal*, 81:51–80, 2024.
- [72] R.E. Showalter. Diffusion in poro-elastic media. *Journal of Mathematical Analysis and Applications*, 251(1):310–340, 2000.
- [73] J.H. Smith and J.A. Humphrey. Interstitial transport and transvascular fluid exchange during infusion into brain and tumor tissue. *Microvasc Res*, 73(1):58–73, 2007.
- [74] Erlend Storvik, Jakub W. Both, Kundan Kumar, Jan M. Nordbotten, and Florin A. Radu. On the optimization of the fixed-stress splitting for Biot’s equations. *International Journal for Numerical Methods in Engineering*, 120(2):179–194, 2019.

- [75] K.H. Støverud, M. Alnæs, H.P. Langtangen, V. Haughton, and K.A. Mardal. Poro-elastic modeling of syringomyelia - a systematic study of the effects of pia mater, central canal, median fissure, white and gray matter on pressure wave propagation and fluid movement within the cervical spinal cord. *Comput Methods Biomech Biomed Engin*, 19(6):686–698, 2016.
- [76] C. Taylor and P. Hood. A numerical solution of the Navier-Stokes equations using the finite element technique. *Internat. J. Comput. & Fluids*, 1(1):73–100, 1973.
- [77] Maria Tchonkova, John Peters, and Stein Sture. A new mixed finite element method for poro-elasticity. *International Journal for Numerical and Analytical Methods in Geomechanics*, 32(6):579–606, 2008.
- [78] K. Terzaghi. *Theoretical Soil Mechanics*. Wiley, New York, 1943.
- [79] P. A. Vermeer and A. Verruijt. An accuracy condition for consolidation by finite elements. *International Journal for Numerical and Analytical Methods in Geomechanics*, 5(1):1–14, 1981.
- [80] H. F. Wang. *Theory of Linear Poroelasticity with Applications to Geomechanics and Hydrogeology*. Princeton University Press, Princeton, 2001.
- [81] Jinchao Xu and Ludmil Zikatanov. A monotone finite element scheme for convection-diffusion equations. *Math. Comp.*, 68(228):1429–1446, 1999.
- [82] Son-Young Yi. A coupling of nonconforming and mixed finite element methods for Biot’s consolidation model. *Numerical Methods for Partial Differential Equations*, 29(5):1749–1777, 2013.
- [83] Son-Young Yi. A study of two modes of locking in poroelasticity. *SIAM Journal on Numerical Analysis*, 55(4):1915–1936, 2017.
- [84] Alexander Ženíšek. The existence and uniqueness theorem in Biot’s consolidation theory. *Aplikace matematiky*, 29(3):194–211, 1984.
- [85] Jijing Zhao, Huangxin Chen, Mingchao Cai, and Shuyu Sun. An optimally convergent parallel splitting algorithm for the multiple-network poroelasticity model. *Journal of Computational Physics*, 539:114214, 2025.